END

FILMED

DTIC

MICROCOPY RESOLUTION TEST CHART
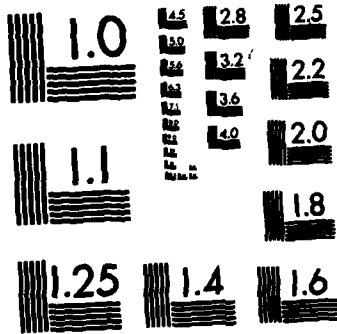NATIONAL BUREAU OF STANDARDS-1963-A

NAVAL POSTGRADUATE SCHOOL
Monterey, California

THESIS

A STUDY OF THE EFFECT OF INTERRUPTED
QUENCHES ON A THERMOMECHANICALLY
PROCESSED HIGH CARBON STEEL

by

Steven A. Barton

October 1982

Thesis Advisor: T. R. McNelley

Approved for public release; distribution unlimited.

DTIC
ELECTED
MAR 1   1983

A

83 02 028 099

#20 - ABSTRACT - (CONTINUED)

rolled material had a higher percentage retained austenite
as well as a higher hardness for all quench interruption
temperatures. This is attributed to a finer starting
microstructure and the retention of refinement throughout
the heat treatment process. Evidence of preferred
orientation was found in the case of the material showing
prior warm rolling.

A Study of the Effect of Interrupted
Quenches on a Thermomechanically
Processed High Carbon Steel

by

Steven A. Barton
Lieutenant, United States Navy
B.S., University of Wisconsin, 1977

Submitted in partial fulfillment of the
requirements for the degree of

MASTER OF SCIENCE IN MECHANICAL ENGINEERING

from the

NAVAL POSTGRADUATE SCHOOL
October 1982

Author: _____

Approved by: _____
Thesis Advisor

_____
Second Reader

_____
Chairman, Department of Mechanical Engineering

_____
Dean of Science and Engineering

ABSTRACT

The effects of short quench interruptions on the percentage retained austenite and the hardness and microstructure were investigated for AISI 52100 steel. Effects were observed for two starting microstructures: an as-received, spheroidize-annealed material, and a fine-grained, warm rolled material. Results indicate that retained austenite and hardness were independent of the quench interruption temperature. The warm rolled material had a higher percentage retained austenite as well as a higher hardness for all quench interruption temperatures. This is attributed to a finer starting micro-structure and the retention of refinement throughout the heat treatment process. Evidence of preferred orientation was found in the case of the material showing prior warm rolling.

TABLE OF CONTENTS

LIST OF TABLES

7

LIST OF FIGURES

ACKNOWLEDGEMENTS

I wish to express my deep appreciation to Professor Terry R. McNelley for the many hours of guidance and assistance he gave me. In addition, I wish to express my truly sincere thanks to my wife, Pamela, and my boy, Kyle, whose continuous support and patience made this research possible.

I. INTRODUCTION

A. PURPOSE

Steels for application in rolling element bearings have received renewed attention in recent years with the advent of still more demanding service conditions in military gas turbines. Such steels typically are high in carbon (e.g., 1.0% C) and contain further alloying additions. One such material, AISI 52100, a 1.0% C - 1.5% Cr alloy, was the material examined in this research. Two areas of particular interest were: (1) the application of a warm rolling process developed by Sherby [Refs. 1,2] to achieve a fine-grained structure that results in improved mechanical properties [Refs. 3-7] and (2) the determination of the retained austenite (RA) content as related to the grain refinement of the warm rolling and the subsequent heat treatment of the material. The RA content of the steel is important as a microstructural feature and is an aspect of the fatigue resistance, ductility, dimensional stability, hardness and strength of the steel.

The present study furthers the research effort in both of these basic areas by investigating the effects of short quench interruptions, most commonly referred to as "marquenching", on the percentage RA, hardness and microstructure for both an as-received (AR), spheroidize-annealed material and a fine-grained, warm rolled (WR) material. Marquenching is employed in current industrial practice, and its purpose primarily is to

11

reduce the effects of large thermal gradients. Furthermore, marquenching temperatures are normally restricted to those below M_s; whereas the present study investigated temperatures above M_s as well. RA measurements were accomplished using X-ray diffraction methods. Although numerous questions remain as to the overall effect of RA in bearing materials, its micro-structural control is of current industrial concern. In addition, although 52100 steel is currently utilized in the as-received, spheroidize-annealed condition, it has already been demonstrated [Refs. 3-7] that the fine-grained structure pro-duced by the Sherby warm rolling process possesses mechanical properties superior to those of the conventionally processed material.

B. BACKGROUND

At present, AISI 52100 is the most widely used steel for rolling element bearing applications. In recent years many improvements in processing have occurred and have resulted in improved microstructural control and hence improved mechani-cal properties. Some of these processing areas are: (1) melt-ing methods, (2) ausforging, (3) marquenching, and (4) RA control.

The most advanced melting technique currently used involves vacuum induction melting followed by consummable electrode vacuum arc remelting. Despite the ability of this process to remove all but trace quantities of non-metallic inclusions, Kar, Horn, and Zackay [Ref. 8] have presented evidence that

12

suggest even trace quantities are instrumental in eventual
failure due to rolling element fatigue. Since economic con-
siderations preclude the use of repeated meltings to further
lower the impurity levels, current technology must accommodate
their presence. Other means must therefore be sought to in-
crease fracture toughness and fatigue resistance.

Coarse carbides are known to have a deleterious effect on
fracture toughness in this steel [Ref. 8]. Normally, heat
treatment of 52100 steel involves incomplete austenitization
at relatively low temperatures, resulting in incomplete disso-
lution of alloy carbides, predominantly Fe-Cr complexes. In
some instances 52100 steel is given an ausforging treatment to
increase the fatigue life by the mechanism of strain-induced
precipitation which results in smaller, more uniformly dis-
persed carbides [Ref. 8].

Marquenching is yet another commonly used method in heat
treatment. Interrupted quenching, martempering and marquench-
ing are all terms used to describe an elevated-temperature
quenching procedure aimed at reducing cracking and minimizing
distortion and residual stresses. Marquenching of steel con-
sists of quenching from the austenitization temperature into
a medium warmer than ambient (typically 200 C) until the
temperature throughout the steel is substantially uniform and
then cooling at a moderate rate to room temperature. The
principal advantage of a marquenching procedure is the lessen-
ing of macroscopic thermal gradients by interrupting the

13

quench at a temperature somewhat higher than the low temperature required to assure a nearly complete martensitic transformation. Using an interrupted quench results in the greatest thermal variations occurring while the steel is in the relatively plastic, austenitic condition. Also, the final transformation with its accompanying volumetric changes occur more nearly at the same time throughout a section. Both of these effects help to reduce the residual stresses and thus diminish the susceptibility to both cracking and distortion. Success in marquenching is based on a knowledge of the transformation characteristics (TTT curves) of the steel. Successful martempering requires a cooling rate sufficient to avoid the nose of the C-curve and thus prevent significant bainite formation. When marquenching 52100, maximum hardness may be obtained in sections as thick as 0.89 cm. and this thickness increased to 2.80 cm. when a center hardness 10 HRC units less than the maximum obtainable is acceptable--which is often the case in bearing steels [Ref. 9]. 52100 steel is normally given a "modified" martemper, that is, the temperature of the interrupted quench is below the martensite start temperature. Common temperatures currently being used range from 245 C down to 175 C and holding times may be as long as several minutes. Conversely, marquenching temperatures in this study were as high as 350 C, and 20 seconds time was used at all temperatures (although the marquenching time necessary was less due to the small thickness of the specimens used).

Control of RA is as-hardened 52100 steel is of critical
importance even though it is not fully understood what per-
centage of RA results in an optimum combination of mechanical
properties. Therefore, a brief review of the complexity of
the effect of RA on mechanical properties is in order.

The presence of RA in a martensitic microstructure will
induce both positive and negative changes in mechanical,
engineering and processing properties of steels. The most
important positive effects that specifically relate to 52100
steel are: (1) RA improves contact fatigue life, bending fatigue
resistance and impact fatigue strength [Ref. 10], (2) RA im-
proves ductility and fracture toughness [Ref. 8], and (3) it
improves the corrosion resistance [Ref. 11]. Some of the
most significant negative effects are: (1) adverse growth of
dimensions and embrittlement of the finished product if it is
subjected to temperatures at which RA can transform to untem-
pered martensite isothermally, (2) RA lowers the compressive
yield and ultimate strengths [Ref. 12], (3) it lowers aggregate
hardness and resistance to scuffing and indentation [Ref. 12],
and (4) it increases susceptibility to burn and heat checking
in grinding operations [Ref. 12]. The significance of each
effect varies with the particular application of the finished
product, thus further compounding the problem. However, nearly
sixty years of continued research and commercial service have
established industry standards which indirectly set percentage
RA by requiring specific mechanical properties for particular
applications.

The principal factors which promote retention of austenite
are the same as those which affect the formation of marten-
site: (1) chemical composition, (2) the lowest temperature
to which the steel is cooled, (3) the rate of cooling, and
(4) austenite grain size. A brief discussion concerning these
will better help to understand microstructural control of RA.
Alloying elements, with carbon being the most effective, tend
to interfere with the martensitic shear transformation and
thus promote the retention of austenite. Also, the marten-
sitic transformation is generally athermal and requires cool-
ing to a specified temperature, M_f (often below room temperature),
to be essentially complete. The following two equations
[Refs. 13,14] are often useful:

$$\%RA = \exp\left[-1.10 \quad 10^{-2} (M_s - T_q)\right] \qquad (1)$$

where T_q is the lowest temperature reached in quenching and
the M_s temperature is given by:

$$M_s(C) = 512 - 453(C) - 16.9(Ni) + 15(Cr) - 9.5(Mo) \qquad (2)$$

$$+ 217(C^2) - 71.5(C)(Mn) - 67.6(C)(Cr)$$

where C is the weight percent of carbon in the allow, Mn the
weight percent of manganese, etc. Austenitic grain size is
yet another factor involved in the percentage RA. A smaller
austenitic grain size results in an increased percentage RA

since smaller grains require a greater strain energy per unit volume to make the slight grain shape changes that occur during the martensitic transformation [Ref. 15]. The method of control that has the greatest applicability to this study is that of cooling rate since marquenching has the overall effect of reducing the cooling rate. Woherle, Clough, and Ansell [Ref. 16] have shown that slower cooling rates provide for greater athermal stabilization of austenite and thus a greater percentage RA. Although there is general acceptance that this athermal stabilization is related to the diffusion of the interstitial solutes carbon and nitrogen [Ref. 16], there are two different models for the mechanism. Briefly, these are that the solute particles interfere with the nucleation of martensite [Ref. 16] or that the solute particles interfere with the bulk transformation or actual growth of the martensite [Ref. 16]. After quenching, tempering and cold deformation will generally reduce the amount of RA present [Ref. 17]. It must also be remembered that there are numerous other factors which indirectly affect the amount of RA through one of the factors previously mentioned. An example of this would be the austenitization temperature which affects the amount of alloying in solution as well as the austenitic grain size.

Increased demands placed on bearing materials such as 52100 steel have spurred renewed interest in revising current processing techniques. Central to this effort has been research directed at reducing residual carbide size. Kar [Ref.

8] observed that the most obvious method of reducing residual carbide size, namely, increasing the time and temperature of austenitization, results in a coaser martensite, a larger percentage RA and greater stress concentrations. Quench cracking and lower fracture toughness thus rule this method out as a viable solution. Stickles [Ref. 18] also proposed a carbide refining heat treatment consisting of high temperature austenitization, isothermal transformation to a bainitic microstructure, and followed by the conventional hardening heat treatment. The final as-hardened microstructure consists of a uniform dispersion of fine carbides with increased amounts of RA. Upon further refrigeration treatments to transform this RA to martensite the structure was found to be harder than that produced by conventional heat treatments.

Another carbide refining process is that developed by Sherby [Refs. 1,2]. This thermomechanical process involves warm rolling through the austenite plus carbide region to break up grain boundary carbide networks, followed by warm rolling below the eutectoid so that the carbides that form upon cooling are finely dispersed and spheroidal. The net result is an as-rolled condition of fine spheroidal carbides in a fine ferrite matrix as opposed to the coarse spheroidize-annealed structure that is commonly used for hardening treatments. Subsequent hardening treatments of warm rolled (WR) materials produce finer austenitic and martensitic microstructures and also result in much more finely dispersed carbides.

18

Numerous studies have followed the advent of the Sherby warm rolling process to determine the effect of a finer as-hardened microstructure on mechanical properties. Chung [Ref. 4] observed that warm rolling improved the fatigue resistance of as-hardened 52100 steel. McCauley [Ref. 6] observed that the refined carbide size and uniform distribution of carbides persist through subsequent hardening treatments and result in an improved fracture toughness over conventionally processed material. Schultz [Ref. 5] investigated the hardening and tempering response of 52100 steel that had been given various warm rolling treatments and found the response to hardening to be faster than conventionally processed material. He found not only do WR materials have an improved tensile strength, but more important to the present study, they have a greater percentage RA for a given hardening treatment. There has also been a considerable amount of research directed at microstructural and mechanical changes that take place during isothermal transformation of austenite to bainite [Refs. 5-7]. These studies indicate that a fine bainitic structure possesses sufficient hardness and improved toughness to make its use practical for bearing applications.

The results of Tufte [Ref. 7] had the greatest influence on the present study. He observed that although the grain size of the thermomechanically processed material remained finer than that of the spheroidize-annealed material for a given heat treatment the carbide refinement was not entirely

19

retained. That is, the residual carbides of the WR material present after heat treatment are comparable in size to those of the conventionally used, spheroidize-annealed, material after heat treatment. However, his most important finding that prompted this study was that both the conventionally processed as well as WR materials possessed little or no RA when given an interrupted quench or isothermal transformation above the martensite start temperature. Although no published research has been performed on the effect of quench interruptions on percentage RA much work has been published concerning athermal stabilization of austenite, or the stabilization of austenite upon continuous cooling. Direct correlations can be made since quench interruptions essentially lower the cooling rate, with higher quench interruption temperatures corresponding to lower cooling rates. Using this correlation the data obtained by Tufte is in conflict with generally accepted behavior. That is, it has been found that slower cooling rates, which correspond to higher quench interruption temperatures, result in greater athermal stabilization of austenite and thus a greater percentage RA [Ref. 16]. This is contrary to Tufte's results which indicate that the higher quench interruption temperatures used, those above M_s, showed less percentage RA. Despite this conflict further research on Tufte's findings were warranted since: (1) the aforementioned correlation may not be entirely valid, and (2) the temperature at which Tufte observed the dramatic change in percentage RA occurred near

20

M_s, a temperature at which dramatic microstructural changes otherwise occur.

..

II. EXPERIMENTAL PROCEDURE

A. MATERIALS AND PROCESSING

All of the material used in this research was vacuum-
induction melted (VIM) and consumable-electrode vacuum-arc
remelted (VAR) AISI 52100 steel, from two separate sources.
The materials are the same as used by Schultz [Ref. 5] and
the designation system utilized here is that which was assigned
by Schultz. All as-received (AR) material was in the form
of 8.9 cm. diameter round bar which had been hot rolled to
size and spheroidize-annealed. The material designated 52100/0
was obtained from Vasco Pacific Steel Co. of El Monte, CA. and
that designated 52100/2 was obtained from Carpenter Steel Co.
of Philadelphia, PA. Chemical analysis was performed by
Anamet Laboratories, Inc. of Berkeley, CA. and the results are
presented in Table I. Examination of this data suggests little
difference between these materials although the 52100/2 material
is higher in carbon content and contains a notable amount of
W. A 25.4 cm. length of the AR 52100/2 material was sectioned
from the original bar, heat treated, and rolled as shown in
Figure 1. This material is designated 52100/0-B. Similarly,
a 25.4 cm. length of the AR 52100/2 material was sectioned
from the original bar, heat treated, and rolled as shown in
Figure 2. This material is designated 52100/2-D. The times
indicated in Figures 1 and 2 have been normalized to time per
inch of specimen thickness or diameter. Since the AR condition

22

TABLE I

Alloy Chemistry
(in Weight Percentage)

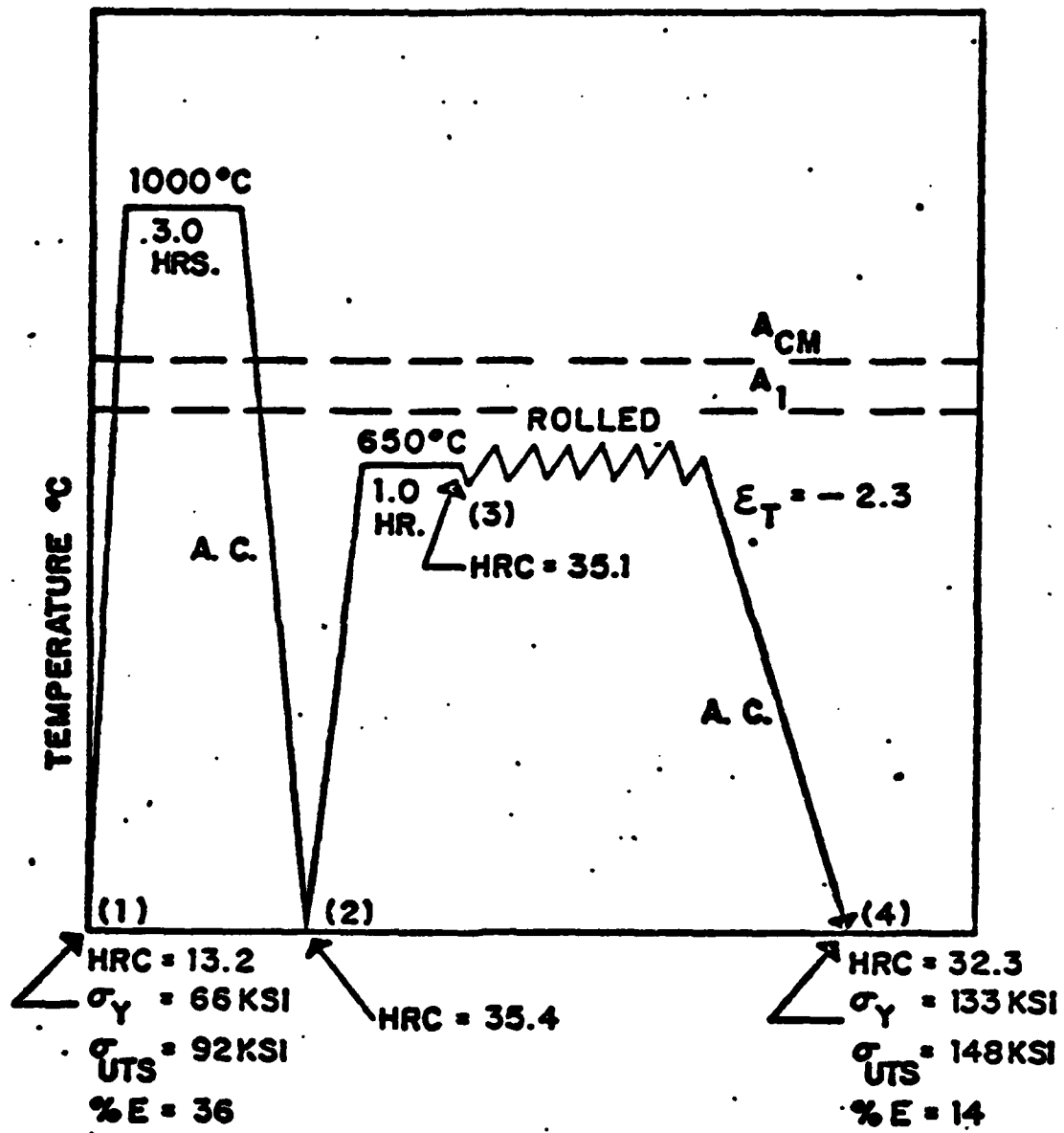| ELEMENT		52100/0 (percent)	52100/2 (percent)
Aluminum	(Al)	0.03	0.03
Carbon	(C)	0.97	1.06
Chromium	(Cr)	1.44	1.50
Columbium	(Cb)	0.008	0.008
Copper	(Cu)	0.11	0.03
Iron	(Fe)	Remainder	Remainder
Lead	(Pb)	<0.005	<0.005
Manganese	(Mn)	0.35	0.38
Molybdenum	(Mo)	0.06	0.04
Nickel	(Ni)	0.18	0.08
Phosphorus	(P)	0.008	0.009
Silicon	(Si)	0.29	0.28
Sulfur	(S)	<0.005	<0.005
Titanium	(Ti)	0.007	0.006
Tungsten	(W)	0.01	0.16
Vanadium	(V)	0.005	0.02

Figure 1. Schematic of Thermomechanical Treatment 52100/0-B.

24
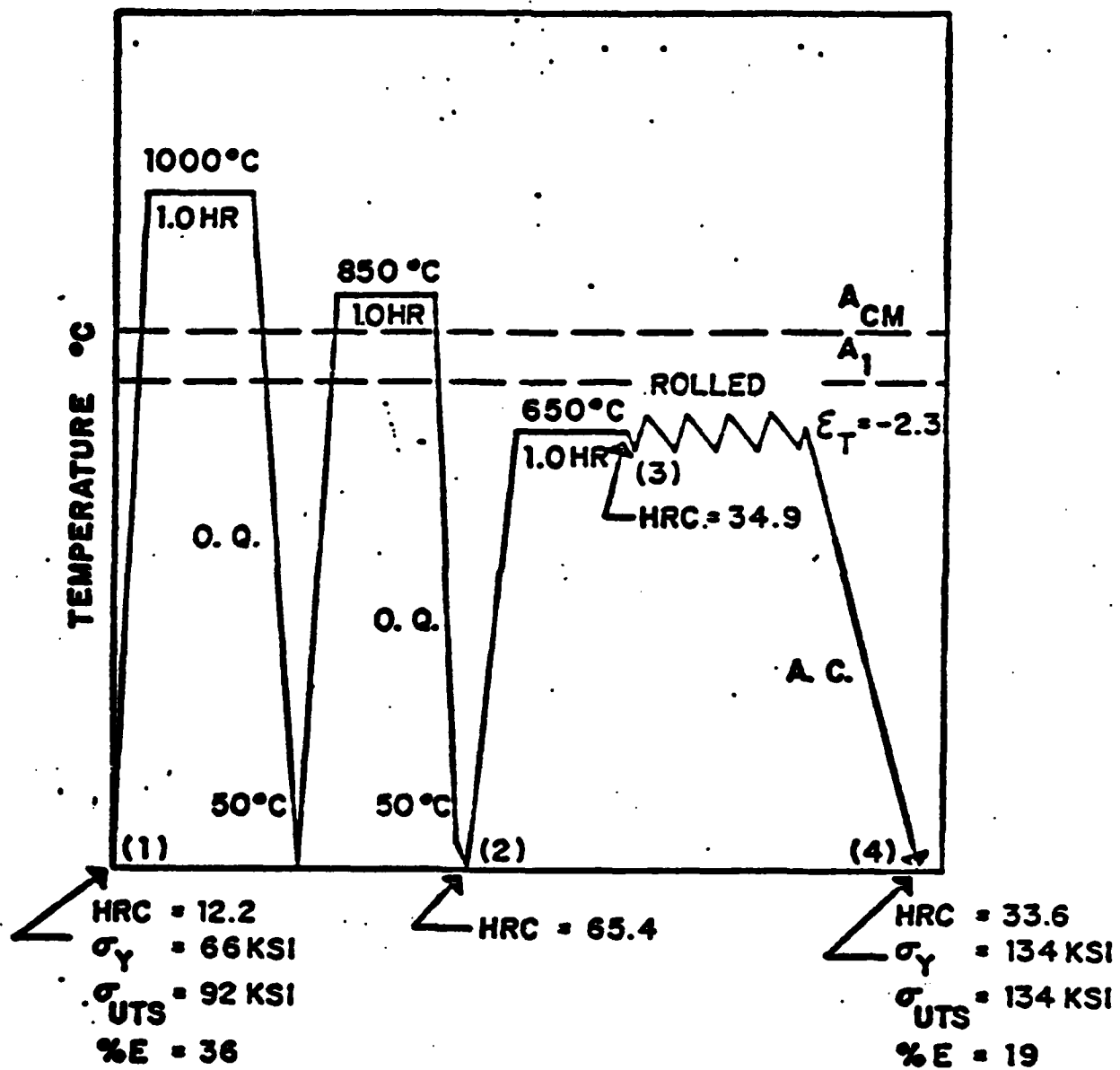
Figure 2. Schematic of Thermomechanical Treatment 52100/2-D.

directly involved in experimentation they are given the designation of 52100/0-AR and 52100/2-AR. For materials 52100/0-B and 52100/2-D the austenitizing treatment and oil quenching was performed by Schultz [Ref. 5] and the final warm rolling was performed by Viking Metallurgical, Inc. of Richmond, CA. Schultz [Ref. 5] gives a more detailed description of materials processing. Prior to heat treatment the 52100/2-AR, 52100/2-D and 52100/0-B materials were machined to provide test coupons of dimensions 2.54 cm. by 1.27 cm. by 0.635 cm. (1.0 in. by 0.5 in. by 0.25 in.). Due to material shortage, the dimensions of 52100/0-AR coupons were 1.27 cm. by 0.953 cm. by 0.635 cm. (0.5 in. by 0.375 in. by 0.25 in.). The coupon size was chosen such that it was thin enough to attain thermal equilibrium during the relatively short quench interruption times.

B. HEAT TREATMENT

Heat treating to accomplish the marquenching consisted of austenitizing in a box-type furnace and then transferring to either a salt bath or a heated oil bath and agitating for 20 seconds, and finally oil quenching to room temperature. This is shown schematically in Figure 3; included on this figure are the nine marquenching temperatures employed. To conduct a heat treatment, four samples, each of one of the four materials/processing conditions to be studied, were wired together. They were then austenitized at 850 C and transferred to a bath at the desired marquenching temperature,

26
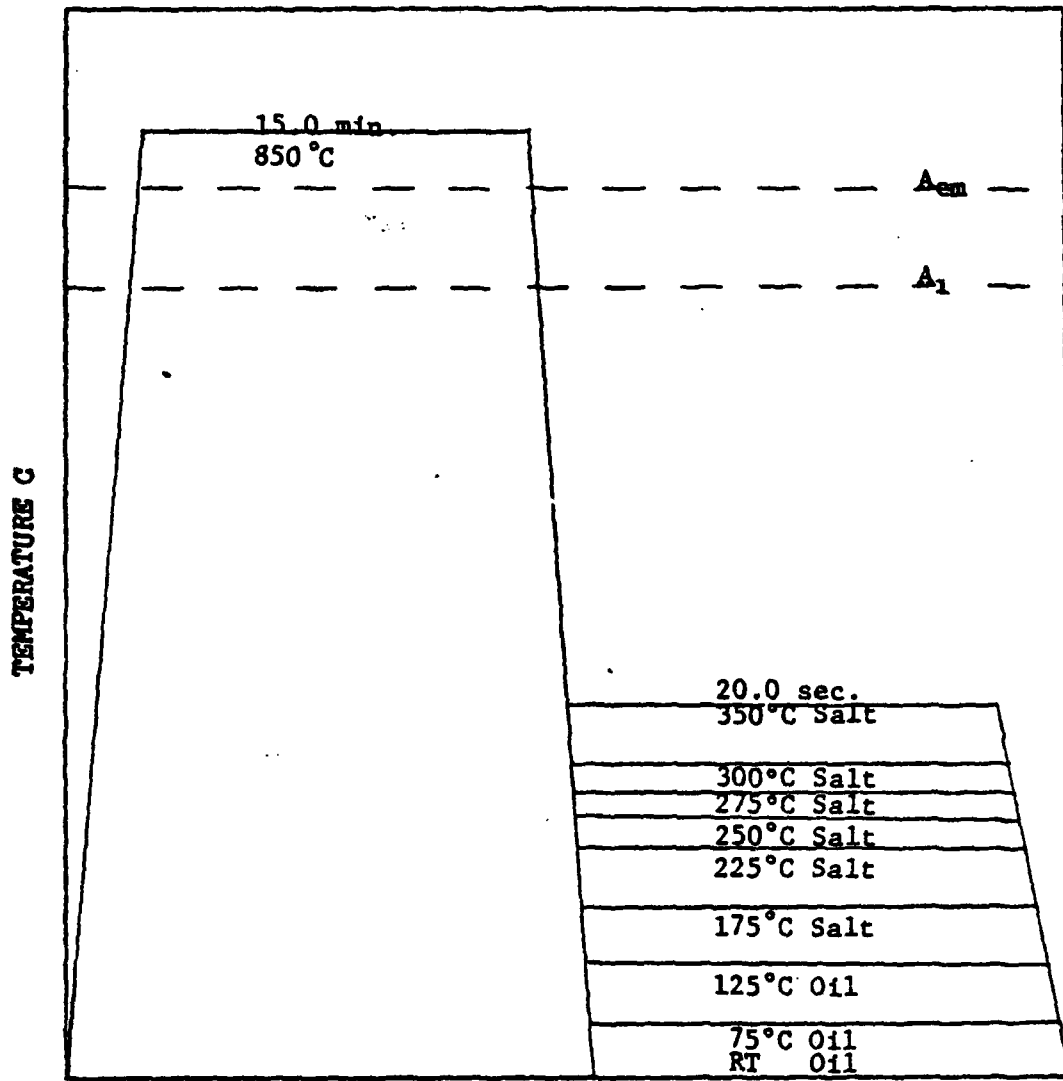
Figure 3.   Schematic of Heat Treatments.

for example 250°C. After 20 seconds, the samples were oil-

quenched to room temperature. Every effort was made to in-

sure the only variable was the marquenching bath temperature.

The measurement of the austenitizing temperature, marquench-

ing temperature, and temperature of final oil quenching medium

were accomplished with the use of thermocouples and digital

pyrometers. For each measurement taken four type "K" chromel-

alumel standard thermocouples were connected to four channels

of a Newport digital pyrometer. The mean value from the four

thermocouples was used and it was generally found that for

all re lings there was close agreement (±3°C). A second

Newport digital pyrometer was then employed to check the

accuracy of the initial readings. An austenitizing temperature

of 850°C (1562°F) with a total heating time of one hour per

inch of thickness (15 min. for the coupon thickness used here)

was chosen since in doing so would facilitate the direct

comparison of data generated here with other available data

on this steel; in fact, most industrial applications utilize

these hardening conditions. The marquenching temperatures

were chosen such that the effects of an interrupted quench

both above and below the martensitie start temperature could

be observed and compared. An interrupted quench time of 20

seconds was used at all marquenching temperatures to ensure

that thermal equilibrium had been attained throughout the

coupon. Tufte [Ref. 7] performed similar marquenching experi-

ments with the interrupted quench time as a variable. The

28

time in the martempering bath was determined based on section thickness, and on the type, temperature, and degree of agitation of the quenching medium. From cooling curves [Ref. 9] based on heat transfer properties of steel in oil and salt bath quenching mediums it was determined that a 20 second interrupted quench would allow for thermal equilibrium conditions to be attained in the center of the coupons. In addition, as indicated in the TTT curve for 52100 steel austenitized at 840°C (Figure 4) the 20 second interrupted quench will avoid the formation of significant amounts of bainite even at higher temperatures.

The broad range of marquenching temperatures necessitated use of two different quenching mediums. For the temperatures of 125°C and below a standard quenching oil was used. For temperatures of 175°C and above a nitrate-nitrite salt bath was used. Since the time required for temperature equalization in oil is four to five times that required in a nitrate-nitrite salt bath at the same temperature [Ref. 9] the preferred interrupted quenching medium over the temperatures attainable by both mediums was the salt bath. The cooling effectiveness of both mediums was increased by vigorous agitation. The final room-temperature quench was performed in oil.

C. OPTICAL MICROSCOPY

Surfaces to be prepared for optical microscopy were obtained by sectioning 0.032 cm. from an end of each coupon

29
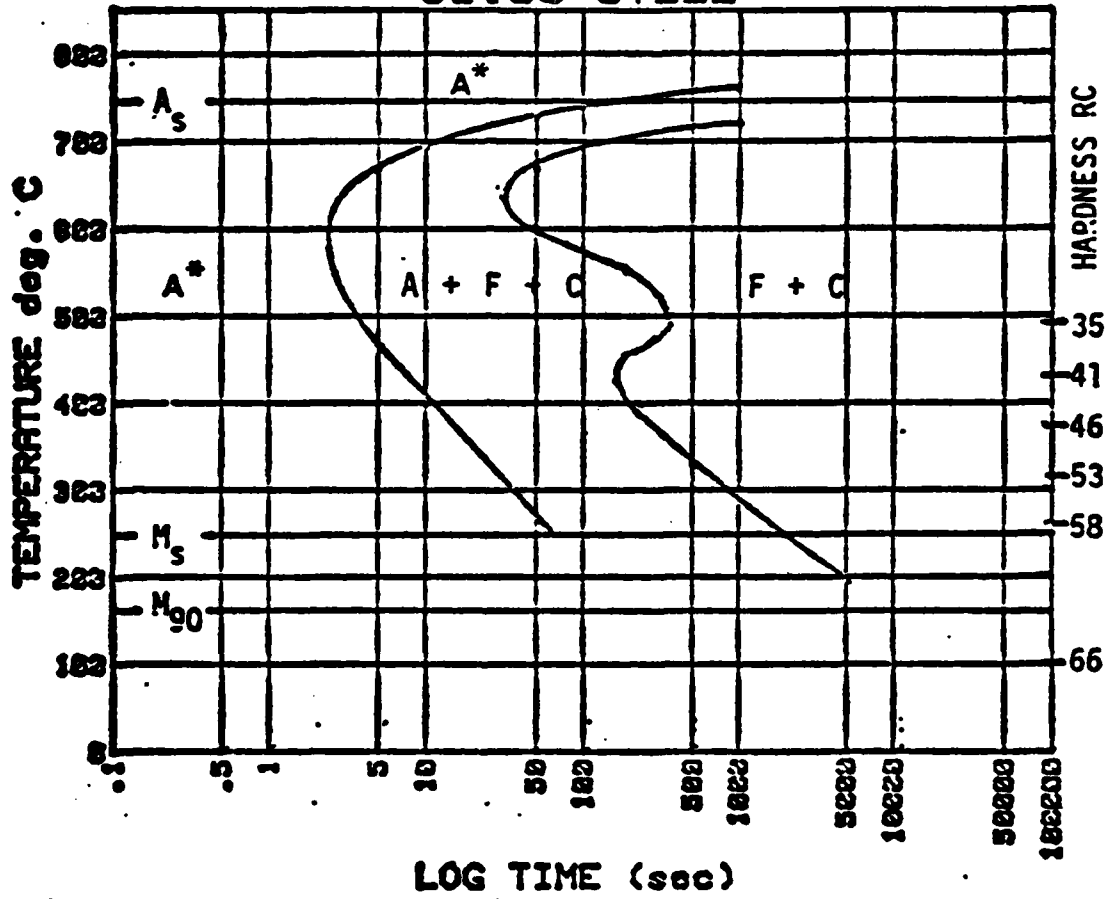
52100 STEEL

Figure 4. Isothermal Transformation Diagram for 52100 Steel

A* - Austenite + undisolved Carbides

using a low speed diamond saw. To facilitate polishing, the samples were mounted in bakelite. The specimens were then mechanically polished through 600 grit paper followed successively by both 1.0 micro Alpha Alumina and 0.05 micron Gamma Alumina micropolish. After washing thoroughly in ethanol the samples were etched in a 2.0% nital solution for times up to 30 seconds. A Zeiss Universal Photomicroscope was utilized for optical microscopy. Magnifications as high as 1600X were employed. This necessitated the use of a 100X oil immersion lens. A Polaroid model 545 land camera was utilized to obtain photomicrographs.

D. ROCKWELL HARDNESS TESTING

All hardness readings were taken using a Wilson Model 1-JR Rockwell Hardness Tester. To obtain accurate individual readings the hardness tester was frequently calibrated using standard Rockwell calibration blocks. In addition, multiple readings were taken to improve the statistical accuracy of each individual hardness measurement. Specifically, the hardness value of each coupon was determined by taking 10 readings, discarding the high and low values, and computing the statistical mean and standard deviation.

Initially, hardness indentations were taken on external surfaces after removing only the external scale using 600 grit paper. Since the Thermolyne box furnace utilized for austenitization did not provide protection from decarburization an additional set of hardness values were taken after

31

removing 0.013 cm. These hardness values were then used for all subsequent experimental analysis.

E. MEASUREMENT OF RA BY X-RAY DIFFRACTION

1. Experimental Apparatus

The retained austenite content was measured using a Philips X-ray diffractometer consisting of a Model 3100 X-ray Generator, Model 42267/0 Goniometer and Philips Data Control and Processor (Figure 5). All measurements were made using a model 1601-4300 Graphite Crystal Diffracted Beam Monochromator in conjunction with a Cu-target X-ray tube. This monochromator serves to filter out all wavelengths except for the Cu K_α and is especially effective in filtering the fluorescent radiation from the Fe of the sample.

The basic focusing geometry of the diffractometer system is illustrated in Figure 6. Of critical importance is the proper alignment of the system. This was verified by a representative of the manufacturer prior to performing the experiment and it was found to be accurate within 0.01 of a degree. Prior to taking diffraction measurements of each sample the compensating slit was adjusted so that the incident beam was confined to the surface to be measured for all 2θ. This was necessary to maintain relative peak intensities as well as to reduce background. A scan range of $49° \leq 2\theta \leq 93°$ was necessary to observe diffraction from the desired crystallographic planes, namely, the (211) and (200) martensite planes and the (311), (220) and (200) austenite planes. A relatively

32
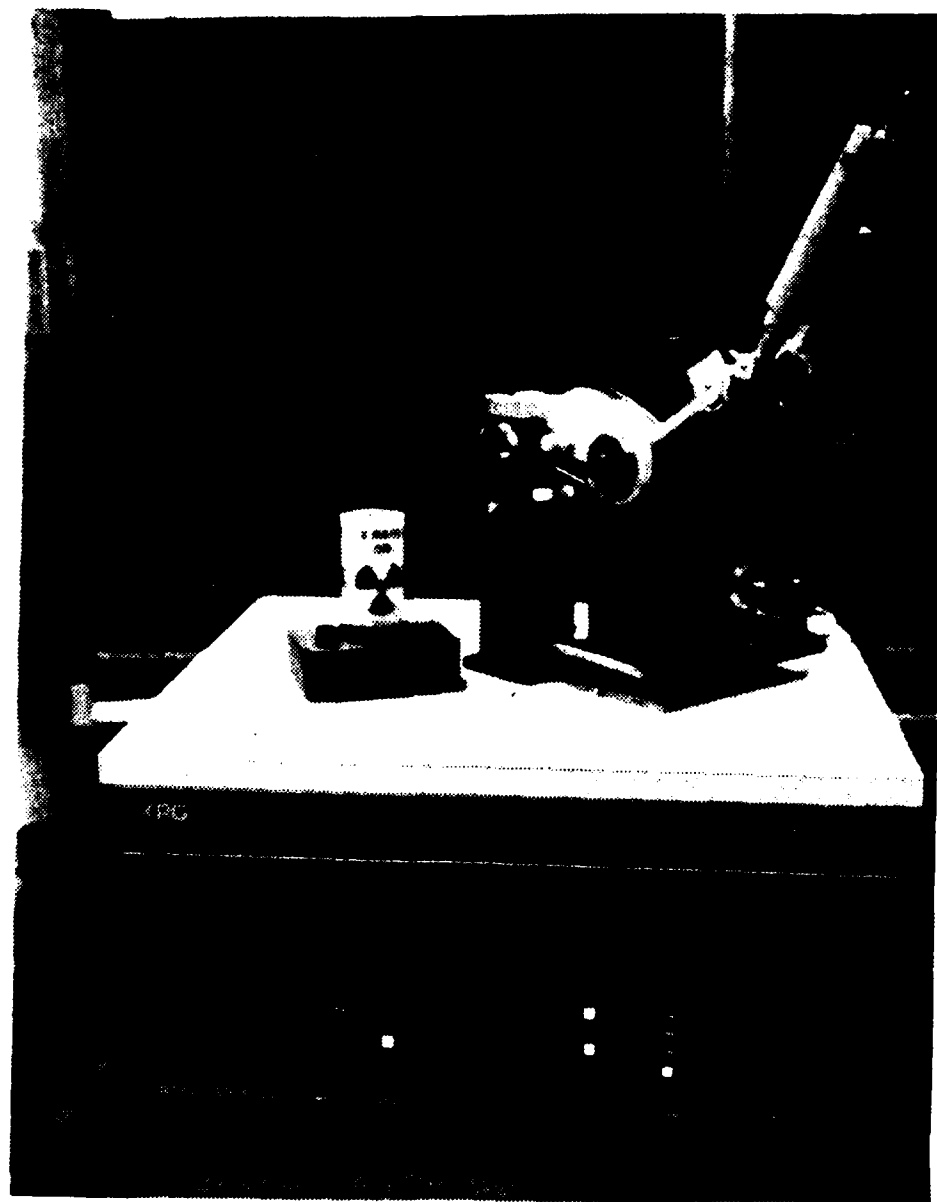
Figure 5.   Philips Model 3100 X-ray Generator and Model 42267
            Goniometer.
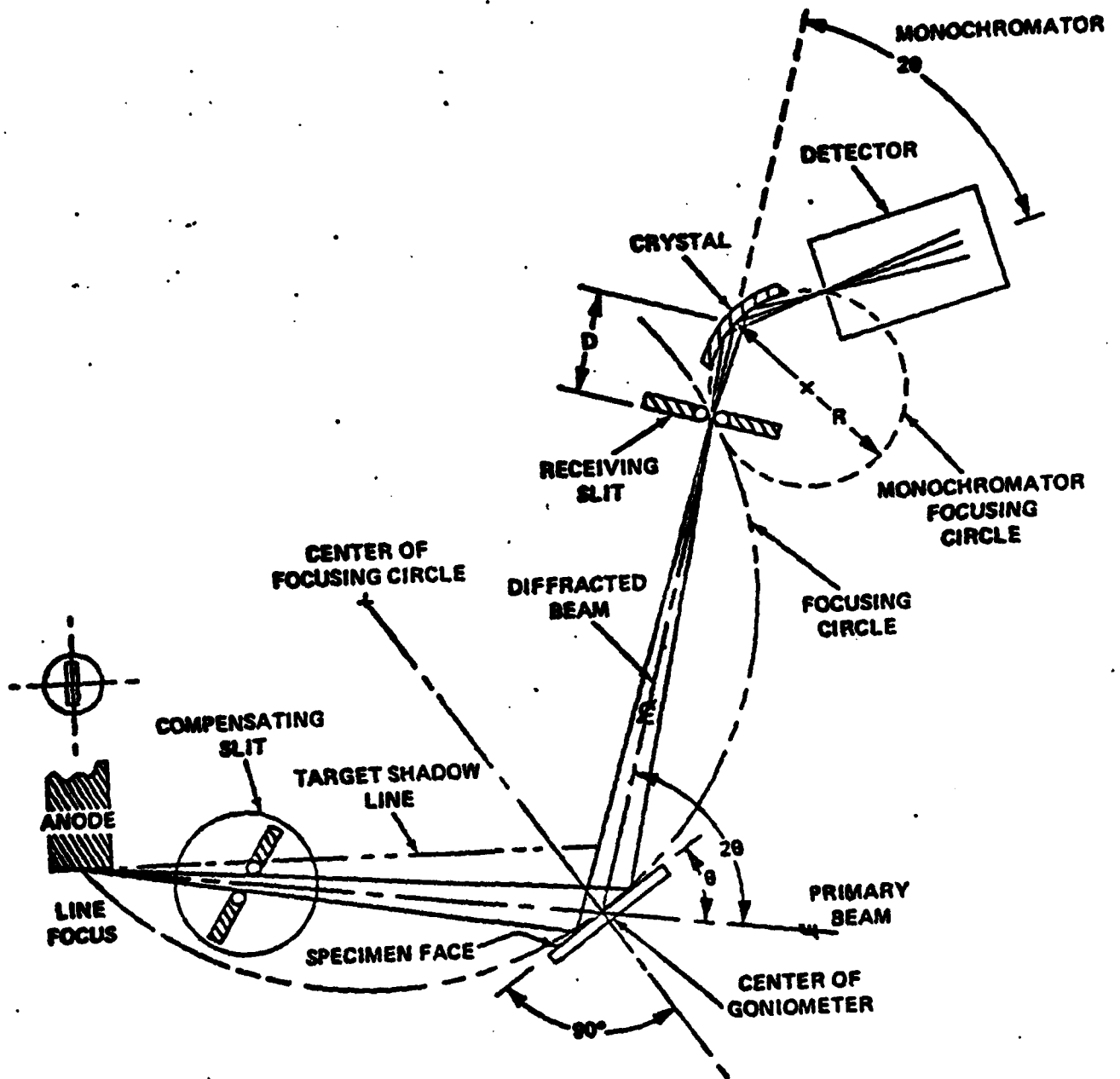
Figure 6. Basic Focusing Geometry of Diffraction System

34

slow scanning rate of 0.5 degrees/min. was necessary to record enough counts to provide sufficiently accurate counting statistics. The receiving slit was set at 0.2 degrees. The graphite crystal monochromator discriminated against unwanted wavelengths originating from numerous sources. With the Cu-target and the Graphite Monochromator, the radiation wavelength λ was taken as 1.54178×10^{-8} cm., the weighted average of the $K_{\alpha 1}$ and $K_{\alpha 2}$ doublet. Tube settings typically were 25 KV and 30 mA to provide a total power of 750 VA, well within the 1800 VA rating of the tube. It was found that increased power settings resulting from use of higher accelerating voltages resulted in a relatively greater increase in background than in peak height and thus degraded peak/background ratio. The data processor was set with a time constant of either 1 or 2 sec. and the gain was adjusted to provide near full-scale deflection for the most intense peak of those of interest, the (211) martensite. The chart speed was set at 0.5 in./min. and with a scan rate of 0.5 degree/min., the chart scale indicated 1.0 degree/in.

2. Specimen Preparation

All surfaces prepared for XRD were taken from the coupon face providing the maximum possible diffracted intensity for improved counting statistics. A surface layer of between 0.013 cm. and 0.025 cm. was removed to insure that the surface exposed to X-rays was not decarburized. In addition, it was essential that all samples be subjected to

the same rate of cooling as this may affect the athermal

stabilization of austenite and hence the amount of RA [Ref.

19]. Since cooling rate varies with distance from the

surface, the removal of nearly equal surface layers ensured

nearly equal cooling rates for all exposed surfaces.

The surfaces were prepared in the following manner.

Approximately 0.01 cm. was removed by dry grinding on 240

grit paper followed by removal of a minimum of 0.003 cm. using

a 600 grit wet grinder. The samples were then mechanically

polished using a 1.0 micron Alpha Alumina micropolish, followed

by a 0.05 micron Gamma Alumina micropolish.

Electropolishing was the final and most important

step in surface preparation. Both stress and thermally in-

duced transformation of RA to martensite may take place in

the surface layers during mechanical polishing. This phenom-

enon was observed in this work by X-ray diffraction measure-

ments indicating little or no RA when conducted on surfaces

resulting from cut-off on a low-speed diamond saw. This is

not surprising, however, in light of the shallow penetration

of Cu K_α radiation in Fe, reported as 2×10^{-4} cm. in Reference

20. A standardized electropolishing technique was utilized

on all samples. This involved 60 sec. in an electrolyte

consisting of 95% glacial acetic acid and 5% perchloric acid.

To provide sufficient current density necessary to avoid

surface etching the electrolytic cell was set at 60 volts.

The procedure removed a minimum of 2.0×10^{-3} cm. which

36

equates to approximately 100 grain diameters of the conventionally processed material. To ensure that this removed all of the surface layer deleteriously affected by mechanical polishing several samples were given another electropolishing treatment in which an additional 5.1×10^{-2} cm. was removed. Subsequent RA measurements on those samples revealed no change in RA when the second electropolishing treatment was performed, thus indicating that the removal of 2.0×10^{-3} cm. is sufficient. An observation that warrants mention here is that the electropolishing procedure produced a dull sheen rather than a bright and shiny finish as might be expected. This is due to the material and is primarily a result of the high carbon content of 52100 steel.

3. Calculating Percentage RA

The (211) and (200) martensite, and the (211), (220) and (200) austenite peaks were scanned to provide data for calculation of RA. Additional data needed for calculation is presented in Table II. The selection of these particular planes provided for: (1) good peak separation (resolution), (2) low Fe_3C peak interference, (3) martensite peak intensities that enabled the smaller austenite peak intensities to be measured with a good degree of accuracy, and (4) a sufficient number of austenite peaks so that in the presence of preferred orientation the measured RA more nearly reflects the actual value.

For all samples the equation used for the calculation of RA was:

TABLE II.

THEORETICAL LINE INTENSITIES (R-VALUES) FOR MARTENSITE AND AUSTENITE PHASES IN STEEL USING COPPER RADIATION

C. Copper Radiation   λ = 1.54178 Å $k_β/k_α$ = .004

Cubic hkl	Tetragonal hkl	d	2θ	$\frac{\sin\theta}{\lambda}$	f_{Fe}	Δf	$(f-\Delta f)$	$|F|^2$	p	Lp	e^{-2M}	$\frac{a_o}{0.2}C$	$\frac{c_o}{1.0}C$	$\frac{a^2}{0.2}C$	$\frac{c^2}{1.0}C$	$\frac{R}{0.2}C$	$\frac{R}{1.0}C$	$\frac{\Sigma R}{1.0C}$
110M		2.027	44.60	0.246	17.4	-1.5	15.9	1011	12	11.31	0.956	2.872		561		232.0		
	110M	2.018	44.91	0.248	17.3	-1.5	15.8	999	8	11.13	0.956		2.854		590		144.1	
	101M	2.002	41.90	0.248	17.5	-1.5	16.0	1020	4	11.72	0.957		2.963		590		77.9	222.0
200M		1.433	65.00	0.348	14.5	-1.5	13.0	676	6	4.64	0.913	2.872		563		32.9		
	200M	1.427	65.40	0.335	14.4	-1.5	12.9	666	4	4.77	0.913		2.854		590		19.7	
	002M	1.491	62.24	0.335	14.0	-1.5	12.3	708	2	5.32	0.920		2.963		590		11.7	31.4
211M		1.170	82.30	0.426	12.9	-1.5	11.4	529	24	3.13	0.873	2.872		563		60.9		
	211M	1.173	82.13	0.426	12.9	-1.5	11.4	528	16	3.13	0.874		2.854		590		32.6	
	112M	1.199	79.99	0.417	13.0	-1.5	11.5	529	8	3.25	0.873		2.962		590		20.5	52.1
220M		1.014	98.90	0.493	11.7	-1.5	10.2	416	12	2.73	0.850	2.872		563		20.6		
	220M	1.009	99.63	0.495	11.7	-1.5	10.2	416	8	2.73	0.836		2.854		590		12.0	
	202M	1.031	96.77	0.495	11.8	-1.5	10.3	412	4	2.73	0.840		2.963		590		6.4	19.2
310M		0.906	116.60	0.552	10.9	-1.5	9.4	353	12	3.16	0.803	2.872		563		19.2		
	310M	0.902	117.33	0.554	10.8	-1.5	9.3	346	4	3.19	0.797		2.854		590		6.0	
	103M	0.811	116.37	0.532	11.1	-1.5	9.6	369	4	2.93	0.811		2.963		590		5.0	
	301M	0.790	116.54	0.552	10.9	-1.5	9.4	353	4	3.15	0.790		2.854		590		6.0	17.9
222M		0.827	137.40	0.604	10.1	-1.5	8.6	296	8	4.69	0.780	2.872		563		16.1		
	222M	0.835	134.56	0.598	10.2	-1.5	8.7	203	6	4.54	0.767		2.856		590			14.3
111A		2.078	43.60	0.241	17.5	-1.5	16.0	4096	8	11.91	0.960	3.564	3.599	2049	2173	782.0	172.6	
200A		1.799	50.80	0.278	16.3	-1.5	14.8	3305	6	8.42	0.944	3.564	3.599	2049	2173	81.6	76.9	
220A		1.272	74.60	0.393	13.5	-1.5	12.0	2304	12	3.66	0.900	•	•	•	•	44.4	42.9	
311A		1.085	90.60	0.463	12.2	-1.5	10.7	1832	24	2.80	0.855	•	•	•	•	52.3	44.4	
222A		1.030	96.0	0.481	11.9	-1.5	10.4	1731	8	2.70	0.850	•	•	•	•	15.7	14.8	
400A		0.899	117.9	0.556	10.5	-1.5	9.3	1304	6	3.22	0.809	•	•	•	•	10.4	9.8	
331A		0.825	137.3	0.606	10.1	-1.5	8.6	1103	24	4.99	0.778	•	•	•	•	53.8	51.7	
420A		0.805	146.5	0.621	9.9	-1.5	8.4	1129	24	6.89	0.762	•	•	•	•	63.5	63.5	

$$V_A = \frac{\frac{1}{n_A} \sum_0^n (I_A^{hkl}/R_A^{hkl})}{\frac{1}{n_M} \sum_0^n (I_M^{hkl}/R_M^{hkl}) + \frac{1}{n_A} \sum_0^n (I_A^{hkl}/R_A^{hkl}) + V_C}$$

where V_A is the volume fraction of RA, V_C is the volume fraction of carbides, n_A and n_M are the numbers of (hkl) lines for which the integrated intensities have been measured, and I^{hkl} and R^{gkl} are the integrated peak intensities and R values, respectively, that correspond to the given (hkl) plane. Since the as-hardened samples contained both martensite, BCT structure, and tempered martensite, BCC structure, the $\sum$R values (Table II) were utilized to account for the summation of areas associated with the martensite doublets. All five peaks previously mentioned were utilized in the computation of V_A for all samples. The preferred orientation existing in the WR samples (52100/0-B and 52100/2-D) necessitated the use of all three austenite peaks and two martensite peaks so that the weighted average of the integrated peak intensities more closely represents the theoretical values. Appendix A, Theoretical Considerations of RA Measurement by XRD, more clearly explains the effect of preferred orientation. Although little preferred orientation existed in the AR samples (52100/0-AR and 52100/2-AR) all five peaks were again used in the computation of V_A. This not only reduced the error associated with the measurement of any given peak but it is felt that a better comparison would then be possible between V_A of the AR and WR materials.

39

The integrated peak intensities were taken from the plot of intensity vs. 2θ by measuring the area above background under each peak with a planimeter. R values corresponding to a carbon content of 1.0% were taken from Reference 20 and are presented in Table II (see Appendix A for further discussion of R values).

III. RESULTS AND DISCUSSION

The results to be presented and discussed were obtained
from samples which had been given an austenitizing and mar-
quenching treatment as previously discussed. The heat
treated samples were then evaluated for RA content as well
as hardness. Additionally, microstructure data was produced
for selected samples. The results and discussion of this
data follow, first by considering the effect of marquenching
temperature on the RA content. Later, the microstructural,
hardness and related data are presented and discussed.

A. RETAINED AUSTENITE

1. Interrupted Quench Temperature

X-ray diffraction techniques were employed to obtain
the RA data. Figures 7-10 show RA, in volume percent, for
the nine marquenching temperatures used. Figures 7 and 8 plot
the two as-received (AR) and the two warm rolled (WR) materials,
respectively. These figures allow examination of the slightly
different alloy compositions for each processing condition.
Figures 9 and 10 display this same data but in a different
fashion by plotting both 52100/0 materials and both 52100/2
materials, respectively; these facilitate examination of the
influence of the processing itself for each alloy.

A first important observation is that the percentage
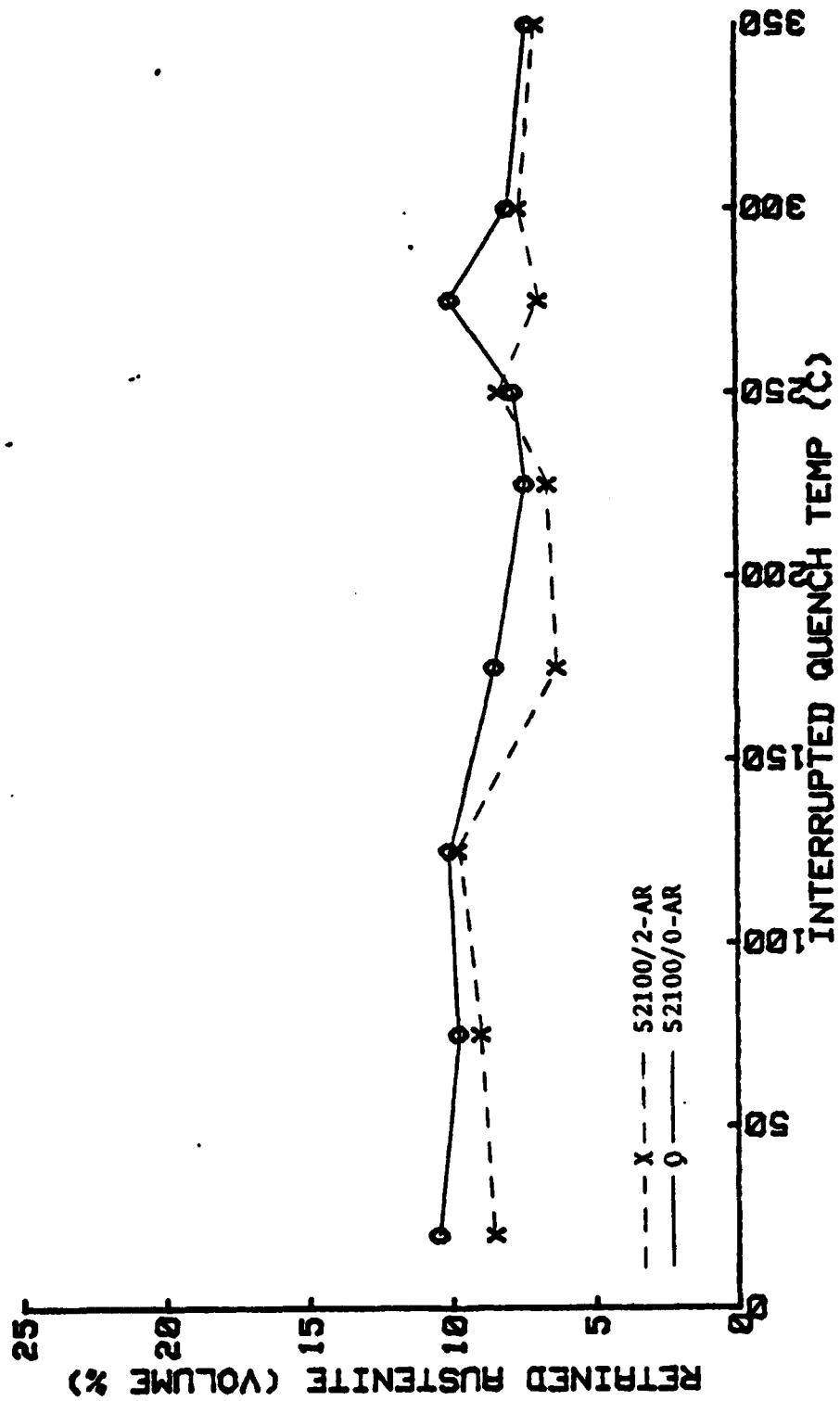RA does not vary with quench interruption temperature. Close

41

Figure 7.   Plot of RA versus quench interruption temperature for both AR materials. Austenitized at 850 C and a 20 second quench interruption at temperatures variously from 20 C to 350 C.
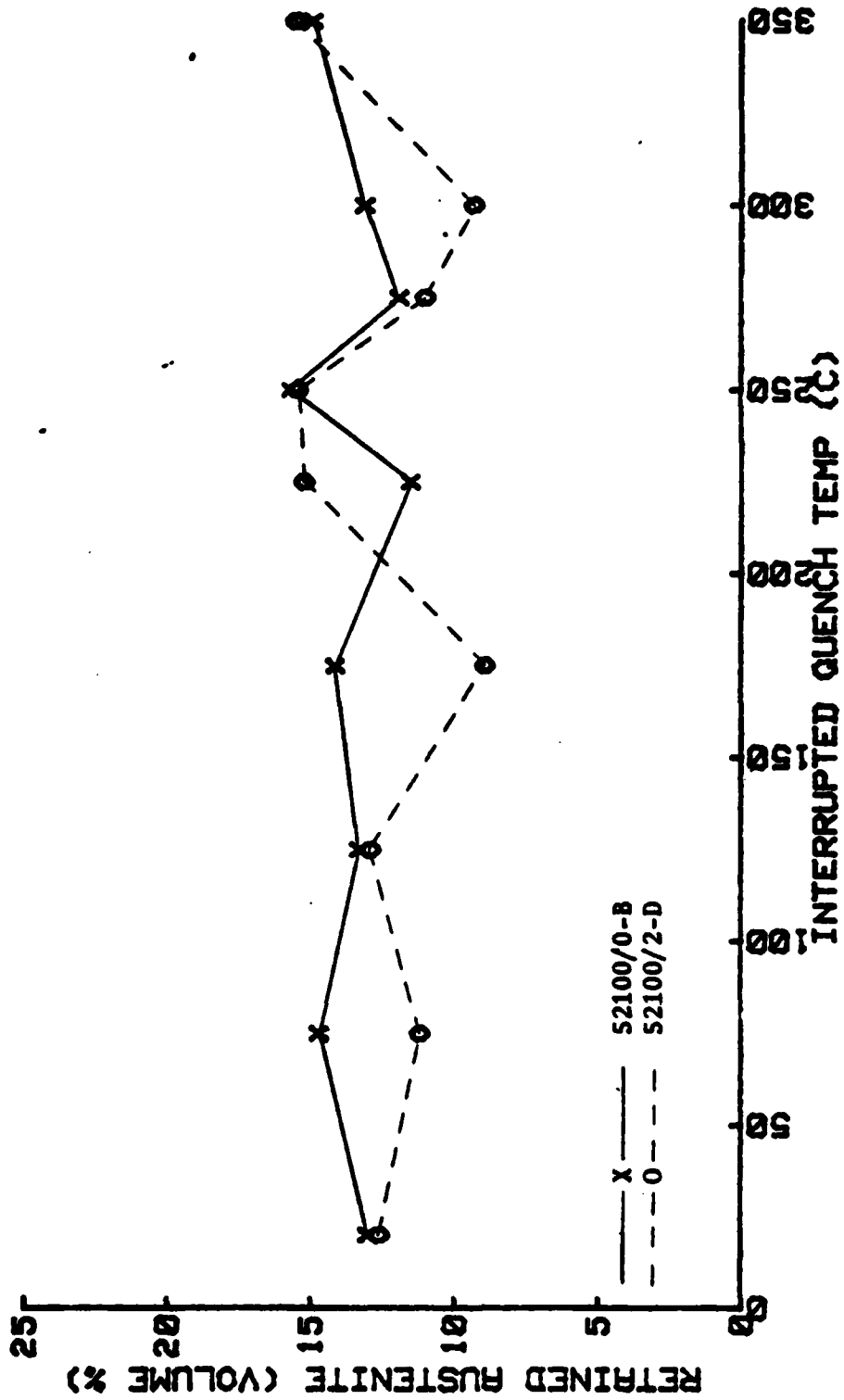
42

Figure 8. Plot of RA versus quench interruption temperature for both WR materials. Austenitized at 850 C and a 20 second quench interruption at temperatures variously from 20 C to 350 C.

43

Figure 9.   Plot of RA versus quench interruption temperature for both 52100/0 materials. Austenitized at 850 C and a 20 second quench interruption at temperatures variously from 20 C to 350 C.
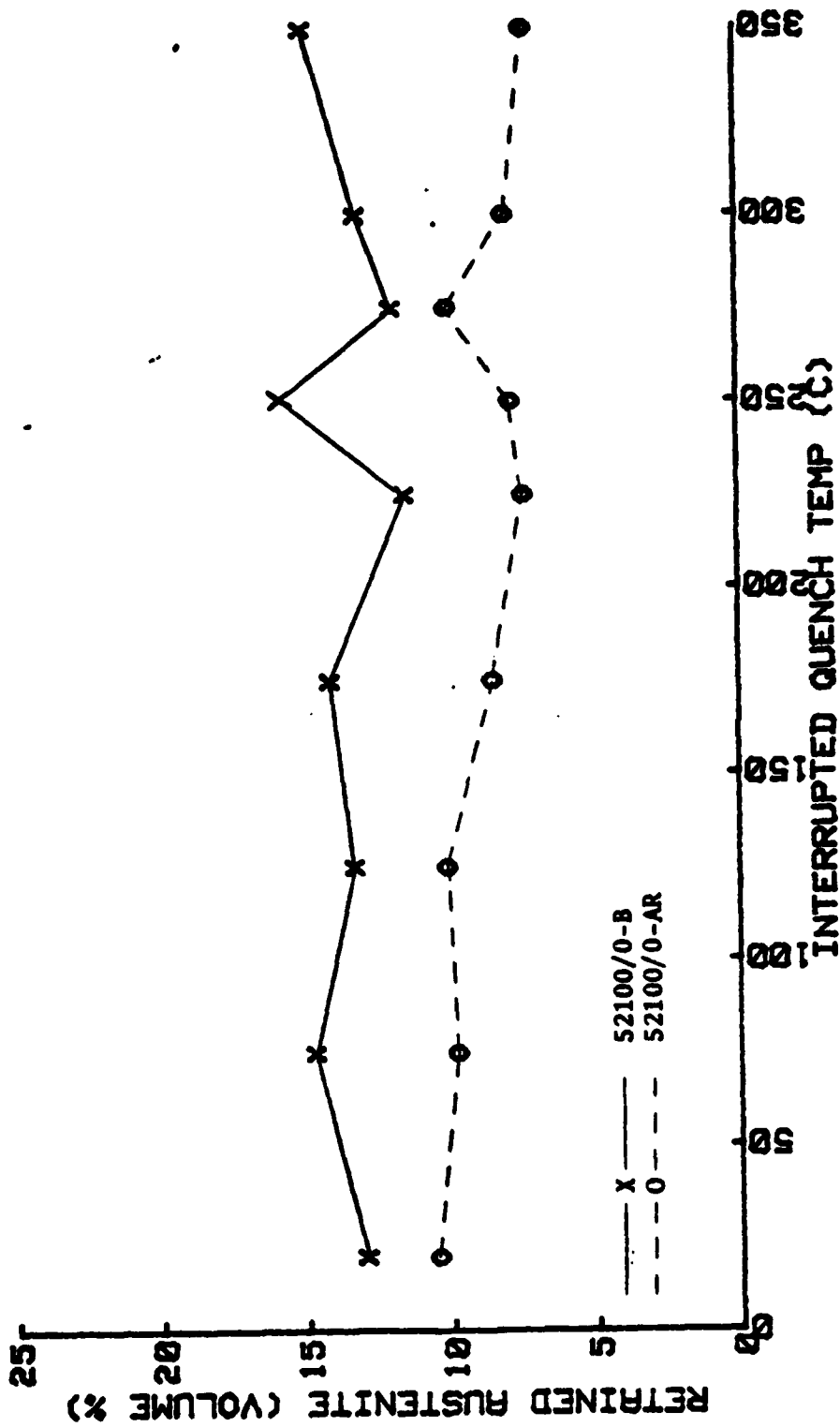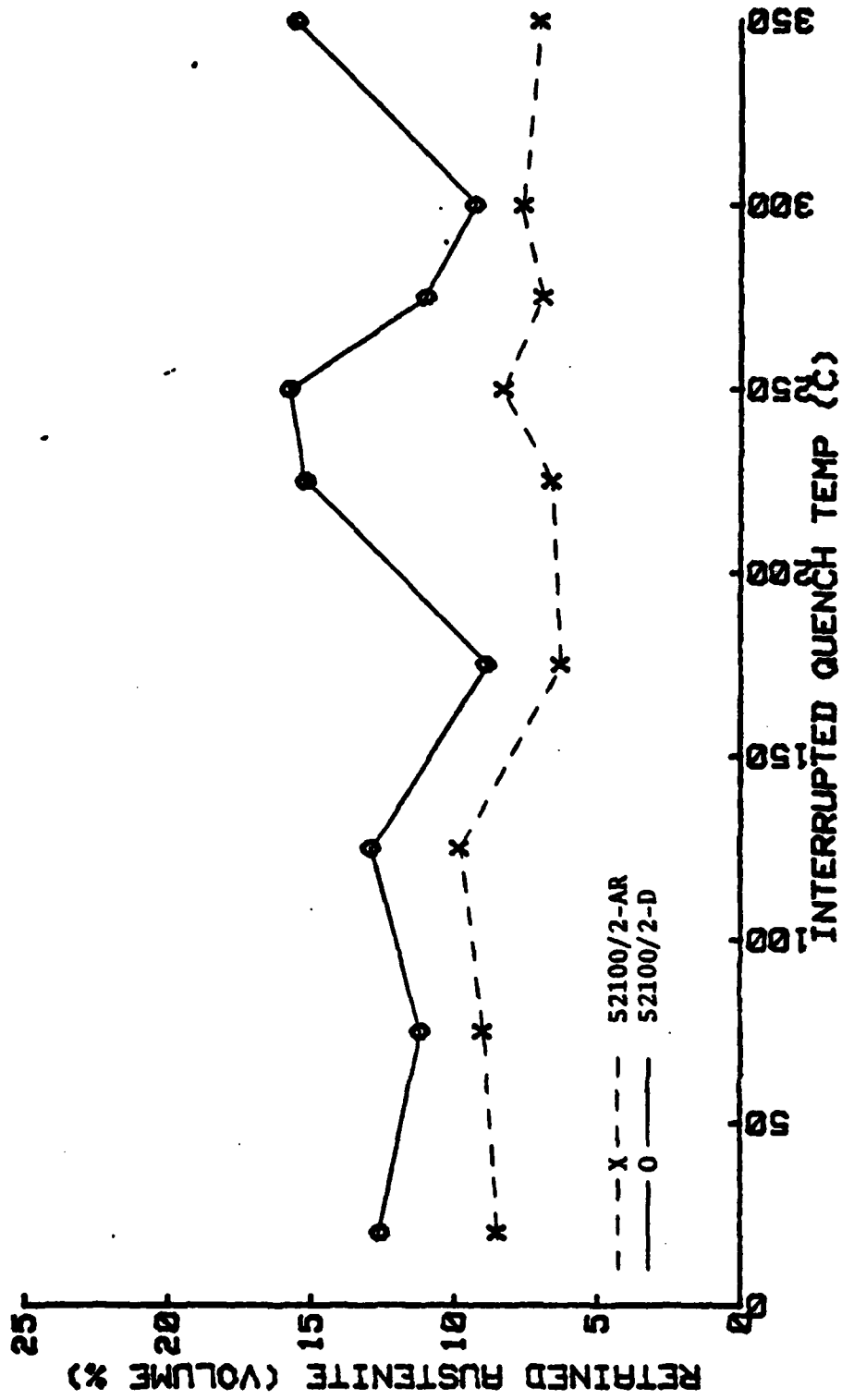
Figure 10. Plot of RA versus quench interruption temperature for both 52100/2 materials. Austenitized at 850 C and a 20 second quench interruption at temperatures variously from 20 C to 350 C.

45

examination of the data reveals that the range of RA values for the four materials is approximately four volume percent of RA. Since the accuracy of RA measurements by X-ray diffraction is typically of the order of ±2.0 volume percent RA [Ref. 20], the apparent variation of RA with quench interruption temperature is within the normal scatter to be expected in the data.

The above experimental result is in accordance with accepted theory [Ref. 19, 21-26] and at variance with the result reported by Tufte [Ref. 7]. One first needs to realize that a quench interruption effectively alters the cooling rate, with higher quench interruption temperatures corresponding to lower cooling rates. Ansell, Donachie and Messler [Ref. 19] and Woehrle, Clough and Ansell [Ref. 16] performed similar experiments to investigate the athermal stabilization of austenite in a wide range of low alloy steels, including AISI 52100 in which the cooling rate was varied during the hardening treatment. Their findings were the same as in the present study, that is, that over the effective cooling rates obtained due to varying the quench interruption temperature, neither the M_s temperature or the percentage RA changed.

Briefly summarized, the results of several studies [Refs. 16,19,26] were that for cooling rates less than 5500 C/sec. there was no observed change in the M_s temperature or the percentage RA. This agrees with the present study since the maximum cooling rate attained, corresponding to the direct

46

quench into room temperature oil, was of the order of 1000-2000 C/sec [Ref. 9]. However, as the cooling rate increased from 5500 C/sec. to 33,000 C/sec. it was found that the M_s temperature increased by approximately 110 C with an accompanying 66 percent decrease in RA content. The mechanism invoked to explain this observation is fairly well understood. With normal cooling rates (actually, any cooling rate less than approximately 5500 C/sec. but fast enough to avoid the formation of pearlite) significant carbon segregation occurs prior to the martensitic transformation. The carbon and other interstitial solutes diffuse to crystallographic imperfections where they interfere with the martensitic transformation, thus stabilizing the austenite. A sufficiently high cooling rate prevents stabilization of austenite by limiting the time for diffusion of the interstitials, raising the M_s temperature and lowering percentage RA. It is believed that the results reported by Tufte [Ref. 7] indicated lower RA content because sample preparation did not remove sufficient disturbed material and thus measured in a layer where RA had been transformed to martensite, e.g., by the cutting/grinding operations conducted.

2. Composition

A detailed analysis of the effects of composition on RA content is useful to further understand the data. The following two equations [Refs. 13,14,27,28] are often used to approximate the M_s temperature and volume percent RA as a function of composition alone:

47

$$\%RA \quad = \quad \exp\left[-1.10 \times 10^{-2}\left(M_s - T_q\right)\right] \tag{1}$$

$$M_s(C) \quad = \quad 512 - 453(C) - 16.9(Ni) + 15(Cr) - 9.5(mo)$$

$$+ \; 217(C^2) - 71.5(C)(Mn) - 67.6(C)(Cr) \tag{2}$$

It has already been discussed how both the M_s temperature and percentage RA vary with cooling rate. Numerous other alloying elements such as W, V, Cu, Co and Al also affect these values and, although not accounted for in Equation (2), they have been included in other empirical relationships [Ref. 20]. These equations also do not consider the austenite grain size [Ref. 15]. The alloying elements considered represent only those in solution in the austenite and this makes the equations difficult to apply. With normal cooling rates, and assuming complete solutioning of alloy elements, Equation (2) is accurate to within ±25 C for a 95% confidence interval [Ref. 27].

Equations (1) and (2) can lend some insight into the percentage RA difference based on the compositional variations of the 52100/0 and 52100/2 materials studied in this research. If one assumes that complete solutioning of alloying elements occurs and the compositions of 52100/0 and 52100/2 from Table I are then substituted into Equations (1) and (2), values of the M_s temperature and percentage RA obtained are much too low and high, respectively, when compared to the value reported in Figures 7-10 and to those commonly obtained [Refs. 16,18,

19]. Stickles [Ref. 18] and Santiago [Ref. 29], among others, suggest an explanation. For heat treatments on a spheroidize-annealed 52100 steel that were nearly identical to those of the present study, it was found that only 0.6 weight percent carbon went into solution during austenitization. The balance remained as residual carbides. This agrees quite well with Equation (2). If the carbon content is left as a variable and the approximate M_s temperature of 250 C [Refs. 7,18] is used together with an average composition from Table I, Equation (2) then yields a value for carbon of 0.7 weight percent. When a carbon content of 0.6 weight percent is used together with an average composition from Table I, Equations (1) and (2) yield values of 264 C and 6.8% for M_s and RA, respectfully. These values are much closer than those obtained assuming all the carbon goes into solution, further supporting the results of Stickles and Santiago.

In Figures 7 and 8 the 52100/0 material was observed to retain a greater percentage of austenite than did the 52100/2 material although this is only a slight trend discernible in the data and the differences are generally within the expected data scatter. From Table I it is seen that one significant compositional difference between the two materials is the greater amounts of both carbon and carbide forming elements, tungsten and vanadium, in the 52100/2 material. Based on the carbon alone one would expect the 52100/2 materials to have a greater percentage RA. It is possible that the carbide forming elements are responsible for the

49

lower RA content in the 52100/2 materials despite their carbon content. Fletcher, Averbach, and Cohen [Ref. 25] observed similar results in their study of the dimensional stability of steel. They theorized that carbide forming elements such as Cr, Mo, W, and V effectively tie up the carbon atoms by forming complex carbides. By reducing the carbon in solution the M_s temperature is raised and the percentage RA is lowered, consistent with the data observed in Figures 7 and 8. Similar results were reported by Ansell, Donachie and Messler [Ref. 19]. They also reported that tungsten raised the M_s temperature but postulated the mechanism to be tungsten atoms restricting carbon diffusion. Another result of their study [Ref. 19] was that nickel enhances carbon diffusion, thus resulting in an increased M_s temperature and decrease percentage RA. Since the 52100/0 material has a greater nickel content than does 52100/2 this observation also is in agreement with Figures 7 and 8.

3. Fineness of the Microstructure

The most significant effect and most obvious difference to be noted in the data of Figures 7-10 is the higher RA content of the WR materials. This is most clearly seen in Figures 9 and 10. Tufte [Ref. 7] and Schultz [Ref. 5] provide microstructural data on these materials in the as-warm-rolled condition and in the as-received condition. They demonstrated that the carbides in the as-received material are 2.0-3.0 μm. in size while those in both warm-rolled materials are 0.1-0.2 μm. in size. The WR materials, possessing

50

this much finer structure, allow a greater amount of carbon to dissolve during the austenitizing treatment by providing shorter diffusional distances for the carbon. The WR materials therefore had a greater effective carbon content during the marquenching treatment and this, in turn, will result in a greater percentage RA. If typical values for the RA content of the WR materials are used in Equation (1), the M_s temperature obtained may be used in Equation (2) to estimate the carbon content of the martensite. The result obtained, 0.7% C, is greater than that similarly obtained using the RA data for AR materials, for which the value obtained is 0.6% C. Both of these values are within the data reported by Stickles [Ref. 18] and Santiago [Ref. 29]. Also, this result is consistent with the results of Differential Thermal Analysis (DTA) data reported by Tufte [Ref. 7], who demonstrated that these WR materials showed greater carbon dissolution on heating than did the corresponding AR materials.

4. Accuracy of Measurements

a. Decomposition at Room Temperature

Due to the decomposition of RA which occurs at room temperature [Refs. 19,21,22,24-26] the results of Figures 7-10 are not representative of the RA percentages which existed immediately after completion of the marquenching procedure. Since RA measurements were taken approximately six weeks after the heat treatments were performed, sufficient time had elapsed to allow the maximum amount of RA to decompose to bainite [Ref. 25]. This determination is based on

51

work by Fletcher, Averbach and Cohen [Ref. 25] who found
that RA decays exponentially with time such that the maximum
RA that decomposes, 25 percent of the initial amount, does
so in approximately 1000 hours, or six weeks. After this
time, the amount of RA remains effectively constant with time.
Although the austenite can be effectively stabilized after
the hardening treatment by performing a low-temperature tem-
pering treatment [Ref. 25] the only procedure which assures
accurate results is to make the RA measurement directly after
the marquenching treatments. The systematic error in RA
values mentioned above is not reflected in Figures 7-10 since
an additional factor, neglection of volume percent carbides
during the computation of RA, has an opposite effect that
nearly balances it.

b. Carbides

Another systematic error, intentionally intro-
duced, was the neglect of residual carbides during the compu-
tation of RA. This was done for two reasons. First, the
volume percent carbides is a very difficult quantity to
determine since it varies with numerous factors such as grain
size, austenitization treatment, etc. Also, the techniques
available for its accurate measurement, i.e., carbide extrac-
tion, X-ray diffraction, etc., are difficult to perform.
Second, it is common practice by the majority of researchers
to neglect its inclusion while calculating the percentage RA
[Ref. 20]. Neglecting it here thus allows closer comparisons

to be made between the results of this experiment and those of others.

The effect of neglecting the carbides in the calculation of RA is to obtain a value which is larger than the actual quantity present. Data by Stickles [Ref. 18] and Tufte [Ref. 7] suggest a carbide content of approximately 7.0 volume percent which is consistent with the proposed carbon solution level of about 0.6 weight percent [Refs. 18, 29]. When RA values were calculated while accounting for the 7.0 volume percent carbides a decrease of approximately 20 percent was realized over the values where carbides were neglected. This 20 percent inflated value obtained by neglecting carbides nearly balances the 25 percent austenite decomposition which occurred at room temperature. The net result is that the values plotted in Figures 7-10 approximately represent the actual percentage RA existing immediately after the marquenching treatment despite the errors due to RA decomposition and omission of the carbide volume fraction.

c. Summary

It has already been reported that RA measurements using X-ray diffraction normally yield results with an accuracy of approximately ±2% RA [Ref. 20]. Figures 7-10 showed random scatter of approximately ±2% RA for each material as the quench interruption temperature varied. Slightly higher scatter, and thus reduced accuracy, was observed for the WR materials primarily due to the presence of high preferred orientation (Appendix A). Indeed, this seemingly poor accuracy

has been reported by others [Refs. 18,19,26] and is normally the reason for performing research on materials containing a high percentage RA [Refs. 16,26] whenever possible. As discussed in previous sections there were numerous possible sources for the introduction of error. These fell into one of three broad areas: (1) instrumental variables, (2) specimen variables, and (3) technique variables. The most significant instrumental errors were the low counting statistics on austenite peaks and the difficulty in separating out background radiation. Only one specimen variable, preferred orientation, introduced significant error. Appendix A covers its effect and, in addition, it will be covered in a later section. And finally, the technique variables were the selection of a proper R value (Appendix A) and the neglect of volume percent carbides in the computation of percentage RA.

Two additional experiments were performed as a check for gross error in RA measurement. First, an unknown sample that had previously been measured for RA content by Lambda Research of Cincinatti, Ohio, was remeasured using the techniques described herein. A value of 5.4% RA was obtained for a sample previously measured as 7.5 ± 1.7%. In addition, two samples used within this experiment were remeasured for RA content at Anamet Laboratories of Berkeley, California using an iron-target X-ray tube. Agreement here was within ±1% RA. A positive assertion that can be made, then, is that no gross errors in RA measurement were made.

B. MICROSTRUCTURE

1. Starting Microstructure

A thorough understanding of experimental results obtained in this research requires knowledge of the starting microstructures. The actual samples given the aforementioned marquenching heat treatments came from the same lots as those used by Schultz [Ref. 5] and Tufte [Ref. 7]. Since both Schultz and Tufte performed detailed analysis on the starting microstructures, namely, 52100/0-AR, 52100/0-B, 52100/2-AR and 52100/2-D, their results mentioned previously in passing, will be presented here. As determined by optical microscopy there were no observable differences between the two as-received (AR) microstructures [Ref. 5]. Both consisted of spheroidal carbies (2-3 μm.) in a ferrite matrix (16-20 μm.). The much finer structure developed during the warm-rolling processes prevented detailed analysis of 52100/0-B and 52100/2-D using optical microscopy. Although both warm-rolled (WR) materials were greatly refined over the AR materials the 52100/2-D material did appear to have a slightly finer structure than that of the 52100/0-B material [Ref. 5]. The finer structure of the 52100/2-D material is probably a result of its double austenitizing cycle and the longer times at austenitizing temperature which allow more complete solu-tioning of carbides. Thin foil electron microscopy revealed a ferrite grain size of 0.6-0.8 μm [Ref. 30]. In addition, carbide extraction electron micrographs indicate residual

carbides are about 0.5 µm. in diameter and the carbides precipitated and refined during warm rolling are about 0.1 to 0.2 µm., in diameter [Ref. 7]. It should be noted, however, that considerable uncertainty exists in measurements of carbide size using the carbide extraction technique [Ref. 7].

2. As-Hardened Microstructure

All samples given the hardening treatments as specified in Figure 3 were prepared for optical microscopy. Using very high magnification (1600X) the general structural response of the materials to the various heat treatments was observable although with some difficulty for the fine structure of the WR materials. A key observation made was that optical microscopy did not indicate any discernible microstructural differences as the quench interruption temperature varied, agreeing quite well with the results of the previous section which showed that percentage RA was independent of quench interruption temperature. For this reason only one micrograph for each of the four as-hardened materials has been included here. Figure 11 depicts the microstructures for 52100/0-AR, 52100/2-AR, 52100/0-B and 52100/2-D which were all quenched directly to room temperature.

Certain microstructural features are common to all the materials, although the fineness of the WR materials makes visual analysis much more difficult. As expected from the transformation characteristics (Figure 4) the microstructures are primarily martensitic with acicular martensite
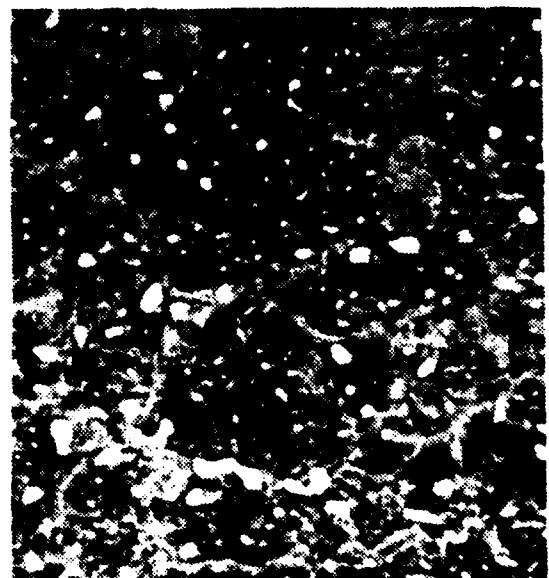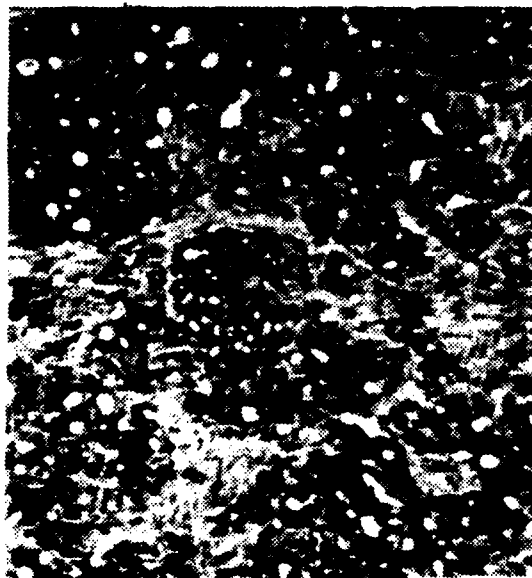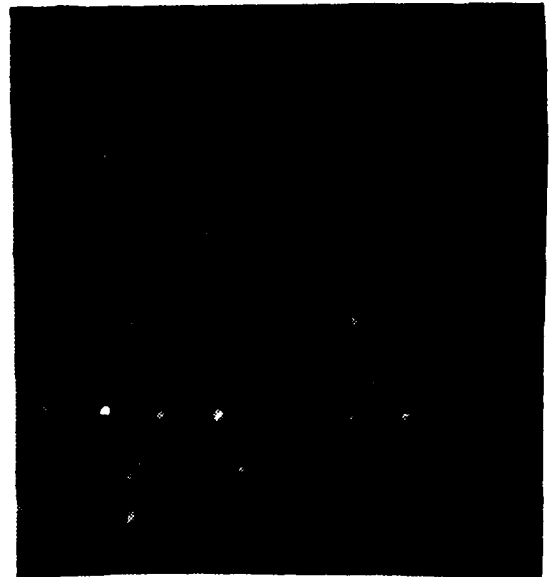
56

Figure 11. Optical Micrographs for As-Hardened 52100/0-B, 52100/2-D, 52100/0-AR and 52100/2-AR Materials Quenched to Room Temperature

57

visible. Using a nital etch, the RA appears as the light colored regions [Ref. 24] and it is visible in all micro-structures as irregularly shaped regions. Spheroidized carbide particles are observable as well as prior austenitic grains boundaries.

The fineness of the WR materials (Figure 11a,b) relative to the AR materials (Figures 11c,d) is the most easily distinguishable difference in microstructures. This indicates that the overall microstructural fineness of the WR materials was retained throughout subsequent hardening treatments. This is expected and has been reported by others [Refs. 7,18]. Included in a discussion of fineness must be carbides which as shown in Figure 11 are smaller for the WR materials. Tufte [Ref. 7], in the conduct of similar experi-ments, reported that during austenitization the residual car-bides of the WR material (carbides which do not go into solu-tion during the austenitization cycle of the thermomechanical treatment) grew to a size comparable with those of the AR material while the carbides precipitated during air cooling and warm rolling retain their fine size. Although this result is not observed in Figure 11 it must be remembered that his work was based on a much more thorough analysis utilizing carbide extraction replicas taken before and after the harden-ing treatments.

Another observation is that the two AR materials (Figures 11c,d) as well as the two WR materials (Figures 11a,b)

appear to have identical microstructures. This is expected in the case of the two AR materials since the starting microstructures were identical. In the case of the two WR materials, the starting microstructure of 52100/2-D was slightly finer than that of 52100/0-B [Ref. 5] and hence its as-hardened microstructure could be expected to be finer. However, the fineness of both WR materials together with the resolution of the micrographs does not allow any microstructural differences to be evident. In addition, it is not expected that the slight compositional variations between the 52100/0 and 52100/2 materials alone would yield differences observable in light microscopy.

A difficult feature to distinguish between the AR materials (Figures 11c,d) and the WR materials (Figures 11a,b) is the RA content. Although easy to observe qualitatively due to its whitish appearance under a nital etch [Ref. 24] it is a most difficult problem to quantitatively determine [Ref. 20]. The difference in percentage RA between either the AR or WR materials from the X-ray diffraction measurements is much too small to be observed in the optical micrographs. In addition, the 5-6 percentage difference in RA in either the 52100/0 or 52100/2 materials observed when comparing the AR and WR states is also not observable, primarily as a result of the fineness of the WR microstructure.

C. HARDNESS

1. Interrupted Quench Temperature

The hardness results are shown in Figures 12-15. None of the four materials show any dependence of hardness on quench interruption temperature. An average range of 1.8 HRC units for the four materials and the inherently poor resolution of hardness for the Rockwell-C scale for hardness values greater than R_C 60 suggest that any apparent variations in hardness can be attributed to normal scatter. The independence of hardness with quench interruption temperature is a result that agrees quite well with both the RA results (Figures 7-10) and the optical micrographs (Figure 11), where it was also found that no variation with quench interruption temperature occurred. Indeed, although the carbon in solution is a primary factor in determining hardness, it has already been noted [Refs. 16,19] that carbon segregation is essentially complete in times far shorter than those governed by the effective cooling rates indirectly obtained in this experiment.

2. Composition

Figures 12 and 13 attempted to show the effect of composition on hardness by plotting both AR materials and both WR materials, respectively. Since the micrographs of Figure 11 indicated nearly identical microstructures for both AR materials as well as both WR materials any hardness differences of Figures 12-15 could be expected to result from compositional variations. In view of the aforementioned
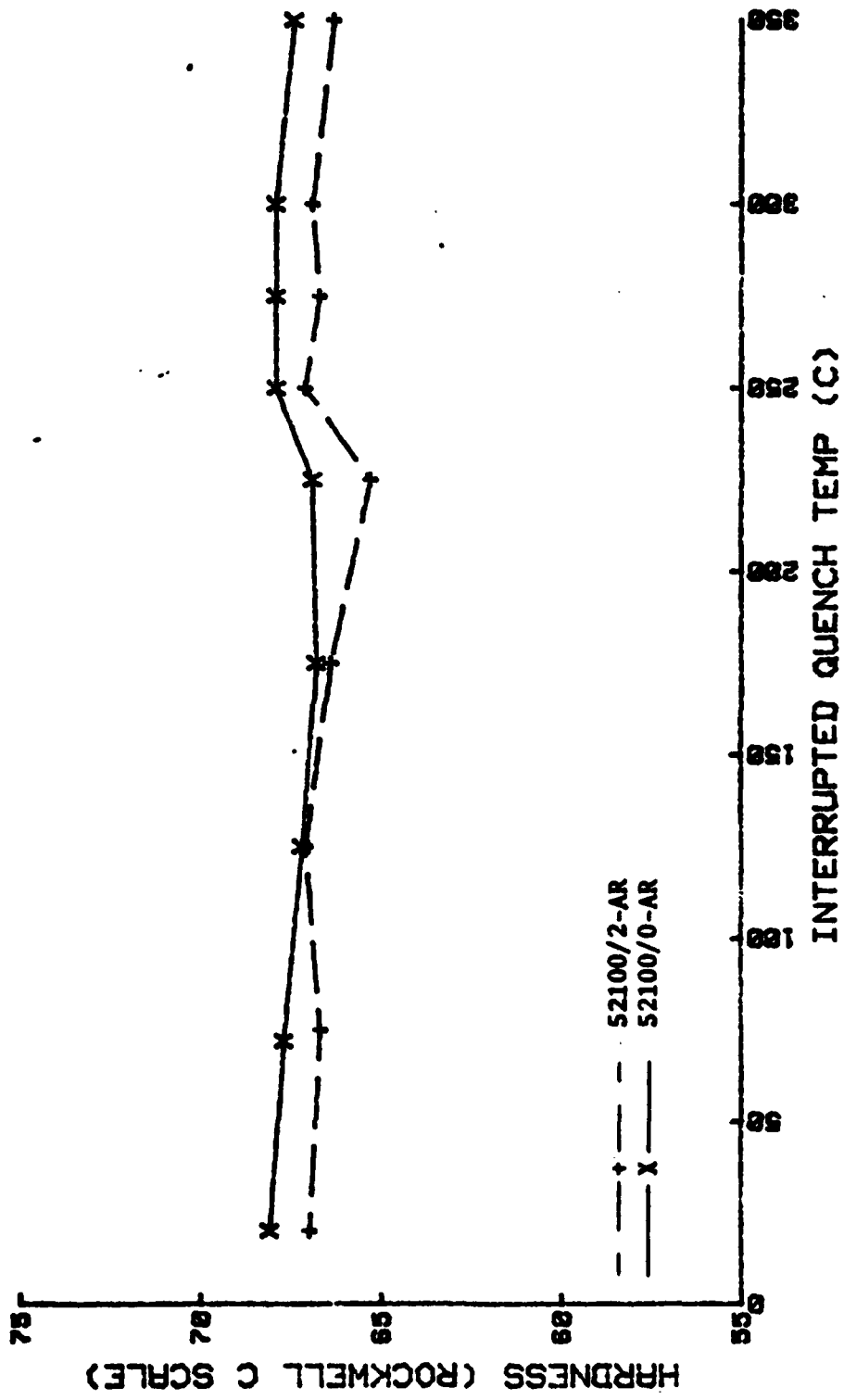
Figure 12. Plot of hardness versus quench interruption temperature for both AR materials. Austenitized at 850 C followed by a 20 second quench interruption at temperatures variously from 20 C to 350 C.
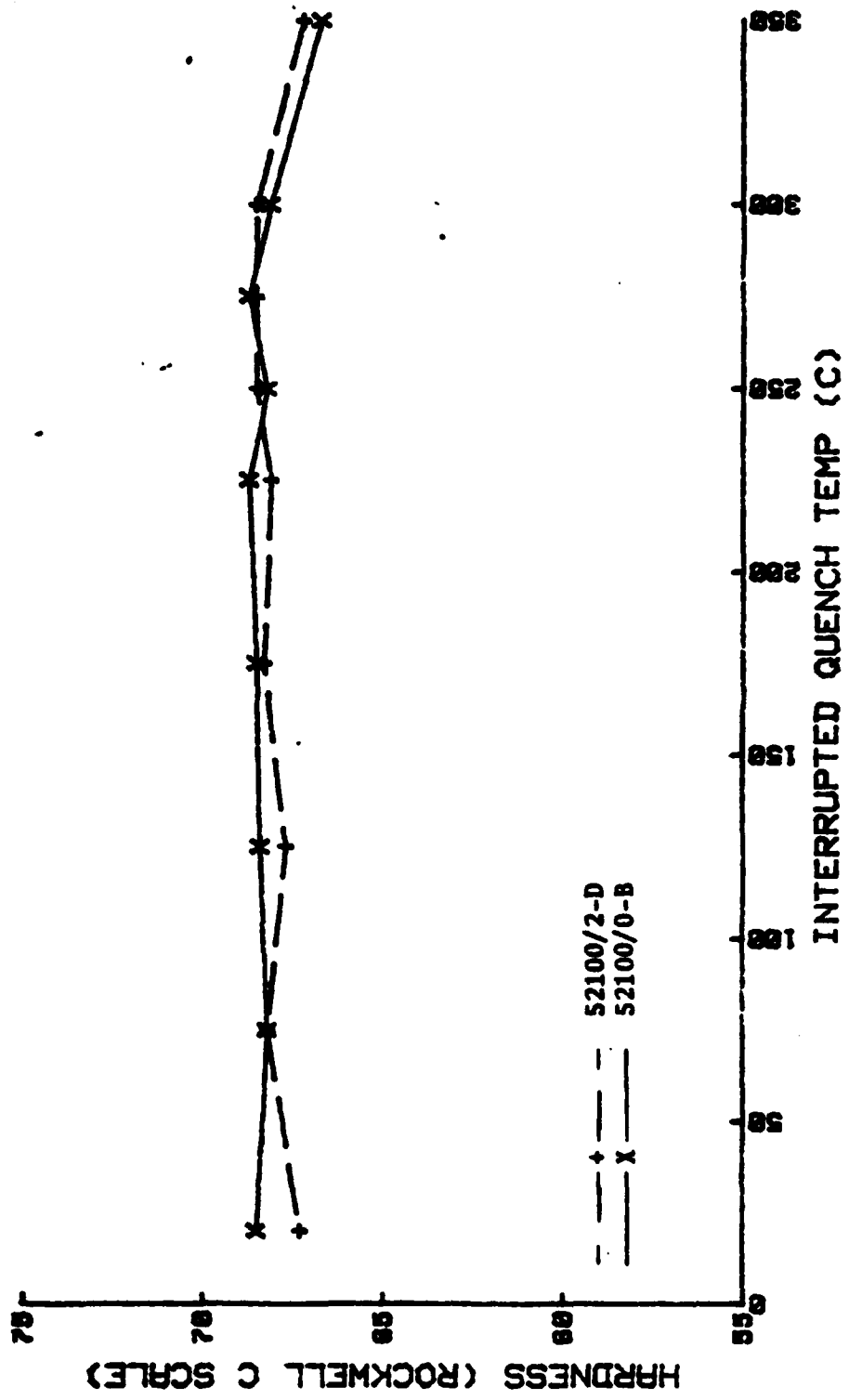
Figure 13. Plot of hardness versus quench interruption temperature for both NR materials. Austenitized at 850 C followed by a 20 second quench interruption at temperatures variously from 20 C to 350 C.

62

Figure 14. Plot of hardness versus quench interruption temperature for both 52100/0. materials. Austenitized at 850 C followed by a 20 second quench interruption at temperatures variously from 20 C to 350 C.

63

Figure 15. Plot of hardness versus quench interruption temperature for both 52I00/2 materials. Austenitized at 850 C followed by a 20 second quench interruption at temperatures variously from 20 C to 350 C.
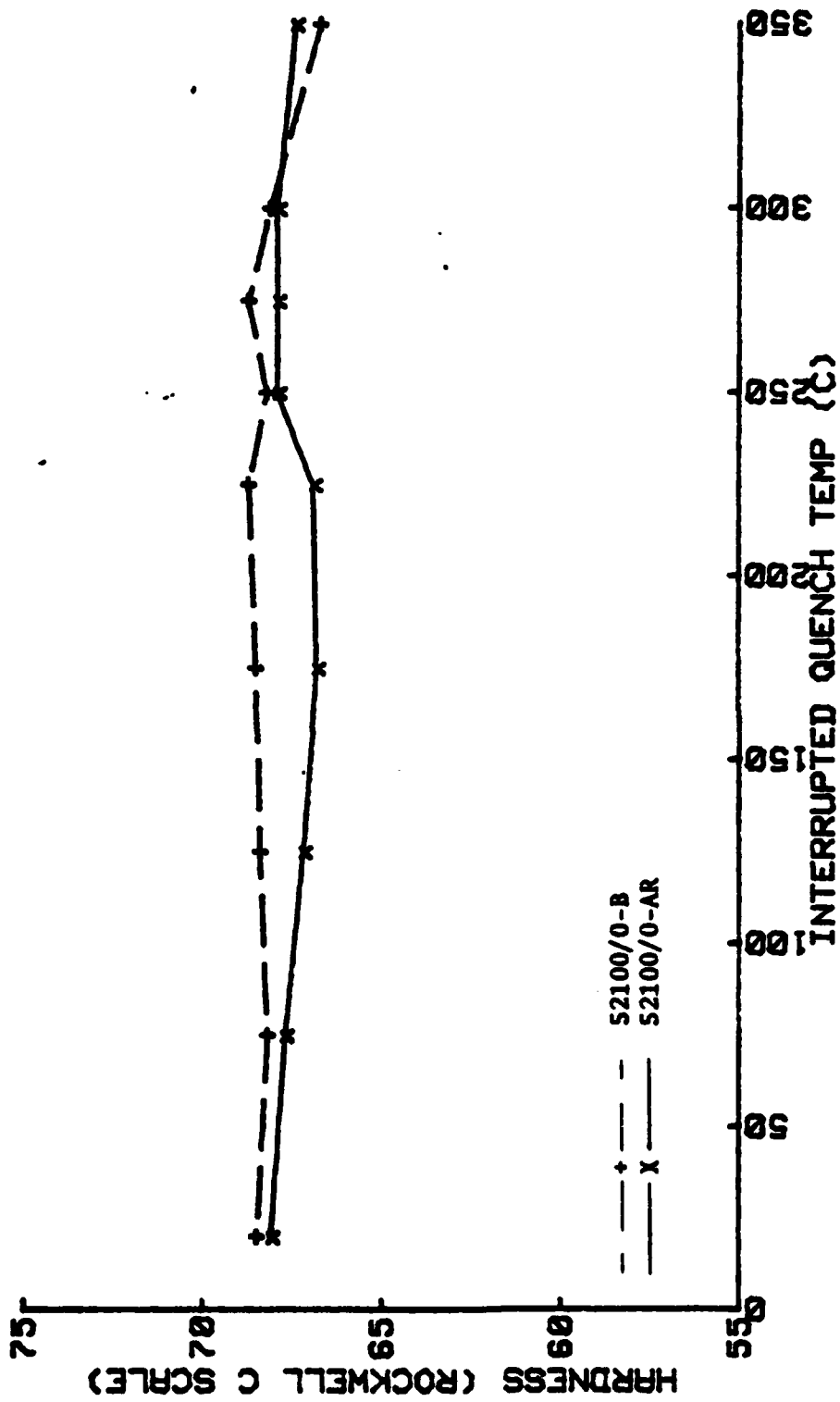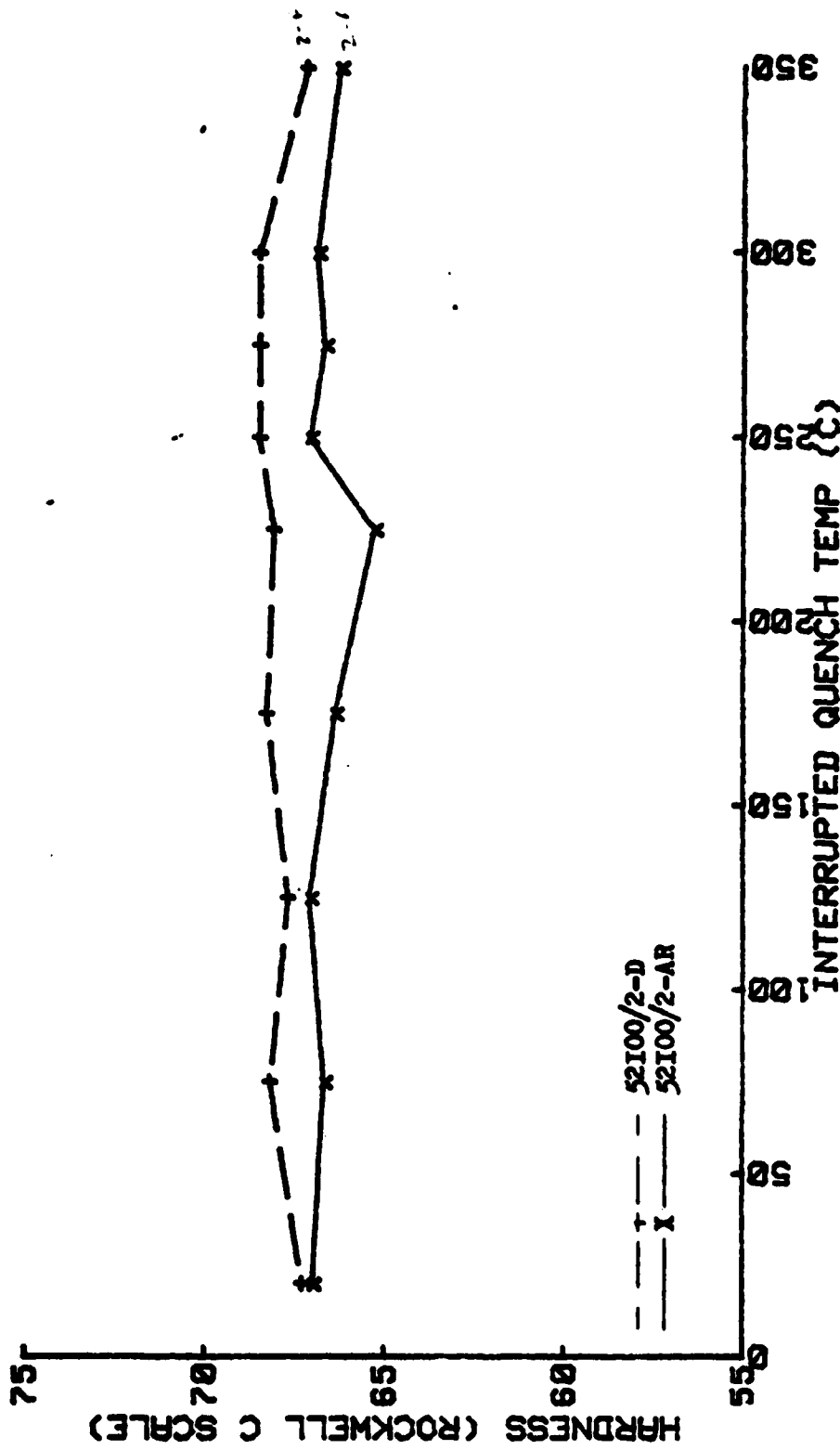
accuracy of the hardness measurements it cannot be stated,
based on examination of Figures 12 and 13 that either material,
52100/0 or 52100/2, has a higher hardness in either the AR
or WR condition. Although most alloying additions increase
hardness it is carbon that has the greatest effect [Ref. 31].
The 52100/2 material, having a greater carbon content (Table
I), might be expected to show a slight increase in hardness.
However, the carbon difference is small and thus not likely
to affect the hardness results.

3. Microstructure

Figures 14 and 15 plot the hardness of the 52100/0
and 52100/2 materials, respectively, for the AR and WR condi-
tions and indicate that the WR materials have higher hard-
ness. This is expected since microstructural fineness tends
to increase strength and hardness. It should be noted, how-
ever, that despite the significant differences in microstruc-
tural fineness between the AR and WR materials indicated by
Figure 11, the differences in hardness are very small,
approximately 1 HRC unit.

Yet another microstructural feature affecting hard-
ness is the presence of RA. RA generally decreases hardness
as does a lower carbon content [Ref. 31: Ch. 6]. Stickles
[Ref. 18], using 52100 steel, clearly showed the combined
effects of percentage RA and carbon content on hardness.
By varying the austenitization time and temperature, Stickles
was able to vary the carbon in solution. An increasing

carbon content was observed to increase both percentage RA and hardness until the carbon content resulted in 15 percent RA. At this point the hardness dropped while the percentage RA continued to rise. This observation was the result of hardness becoming less sensitive to carbon content above about 0.6% C [Ref. 31].

In making hardness-RA comparisons, several observations can be made. Neither the percentage RA (Figures 7-10) or the hardness (Figures 12-15) were determined to vary with quench interruption temperature. Close examination of the individual percentage RA data points with the hardness data points revealed no correlation as the quench interruption temperature varied. As discussed above, since percentage RA and hardness are interdependent this result is expected. This further lends credence to the conclusion that the variations in the percentage RA for each material are a result of normal experimental scatter. If RA did vary systematically with quench interruption temperature by as much as 4 percent RA, then the trend would have been detectable by hardness as well.

Another hardness-RA comparison that can be made is based on microstructural fineness. Figures 9, 10, 14 and 15 show that the fine-grained, WR materials have a greater hardness as well as a greater percentage RA than do the coarser grained, AR materials. This observation also is in agreement with the results of Stickles [Ref. 18]. Since the carbon in solution was approximately 0.6% [Refs. 18,29] the hardness

was still sensitive to carbon fluctuations. The finer struc-
ture of the WR materials allows greater solutioning of carbon
with accompanying increases in both hardness and percentage
RA.

D. PREFERRED ORIENTATION

From measurements of the integrated intensities of the
austenite (200), (220) and (311) peaks it was determined that
the WR materials maintained at least some texturing developed
during the warm rolling processes (Figures 1,2). As detailed
in Appendix A, the integrated intensities of austenite peaks
provide a qualitative measure of the degree of preferred
orientation present in the microstructure. In all AR speci-
mens where no lower-temperature mechanical working was per-
formed, there was no apparent preferred orientation. For
the WR specimens, where mechanical working was conducted as
indicated in Figures 1 and 2, there always existed a moderate
degree of preferred orientation. Clearly, despite the subse-
quent austenitization and hardening treatments the WR materials
maintained some degree of their prior texturing.

IV. CONCLUSIONS AND RECOMMENDATIONS

Based on the experimental observations and results the following conclusions are drawn:

1. The as-hardened microstructure of the WR materials was significantly finer than that of the AR materials.

2. The fine-grained WR materials exhibited both a higher hardness and a higher percentage RA.

3. The variation of quench interruption temperature had no effect on the percentage RA, hardness and microstructure for both the AR and WR materials.

4. Despite having a greater carbon content the 52100/2 materials, which also had a greater amount of carbide forming elements (V and W), possessed a larger percentage RA than the 52100/0 materials.

5. Preferred orientation of the WR materials persists through austenitization and subsequent marquenching treatments.

Recommendations for further research are:

1. Study the effect of RA decomposition at room temperature.

2. Research the ability of carbide forming elements (W, V, Cr, Ti, and Mo) to control the carbon in solution for given austenitization conditions.

3. A more detailed analysis using X-ray diffraction to determine the degree of preferred orientation of the WR materials which persists through austenitization and subsequent hardening quench.

4. Attempt to determine directly, for example by X-ray diffraction, the degree of carbon solutioning during heat treatment of both the grain-refined WR material and the as-received material.

APPENDIX A

THEORETICAL CONSIDERATIONS OF RA MEASUREMENT
BY X-RAY DIFFRACTION

Quantitative determination of the relative volume frac-
tions of martensite and RA can be obtained from the plot
of intensity vs. 2θ because the X-ray intensity diffracted
from each phase is proportional to the volume fraction of
that phase. Furthermore, for a completely random arrangement
of grains the diffracted intensity from any single (hkl)
plane within that phase is also proportional to the volume
fraction of that phase. Thus in the absence of preferred
orientation measurement of the integrated intensity of just
one austenite and one martensite (hkl) line can establish
the volume fraction of that phase.

If texturing in the sample exists, crystallographic align-
ment causes those planes that happen to satisfy the Bragg
angle condition to have larger integrated peak intensities.
The use, then, of a single austenite and martensite plane no
longer gives accurate results.

A quantitative measure of preferred orientation is ob-
tained by comparing the measured integrated intensity ratio
of any two austenite lines I_{A1}/I_{A2} with the calculated ratio
R_{A1}/R_{A2} which defines the theoretical intensity ratio for the
two lines when random orientation exists. When the deviation
of I_{A1}/I_{A2} from R_{A1}/R_{A2} is <20%, <200%, and >200% the degree

of preferred orientation is said to be light, moderate and severe, respectively [Ref. 20].

When a high degree of preferred orientation exists certain (hkl) peaks may not even be observable. This would occur if a high proportion of the corresponding (hkl) planes lie perpendicular to the specimen surface and Bragg reflections are not produced. The error due to texturing may be reduced by using as many (hkl) peaks as possible since the absence of some peaks will naturally result in the predominance of others though not in equal relative amounts since this depends on crystallographic structure and orientation. The error associated with severe preferred orientation can be reduced by the use of a tilting and rotating stage.

Although R values used for computations are normally taken from prepared tables, they may be calculated from theoretical considerations by using the following equation:

$$R^{hkl} = \frac{1}{V^2}(|FF| p \; LP \; e^{-2M})$$

where V is the volume of the unit cell, $|FF|$ is the structure factor times its complex conjugate, p is the multiplicity factor of the (hkl) reflection, LP is the combined Lorentz-polarization factor and e^{-2M} is the Debye-Waller temperature factor. The reader is referred to [Ref. 20] for more detailed discussion. The significance of R is that it is proportional to the integrated peak intensity which should be

diffracted by a specific (hkl) crystallographic plane when 100% of that phase exists and no preferred orientation is present.

R values depend principally upon the chemical composition of the steel and the actual amount of carbon in solution. It is the difficulty in determining the actual amount of carbon in solution which makes the selection of the proper R value such an arduous task. For example, carbon within a single specimen may not be distributed equally between the austenite and martensite phases. In addition, time and temperature of both austenitization and tempering, as well as the amount and type of carbide forming elements, greatly effect the degree of carbon solution.

There are also theoretical difficulties in calculating R values. Uncertainty of dependence of atomic scattering factors on the 2θ angle, size of dispersion corrections, influence of the temperature factor, and the true lattice parameter add additional systematic error. These and other sources of error can add up to unpredictable variations of ±5% in R values, which corresponds to about ±0.6% austenite in a steel containing 20% RA. In light of the overall accuracy of measuring RA by X-ray diffraction methods, this systematic error is acceptably small.

LIST OF REFERENCES

1. Sherby, O. D., and others, "Development of Fine Spheroidized Structures by Warm Rolling of High Carbon Steels," Trans. of the ASM, v. 62, 1969.

2. Third Semi-annual Progress Report to Advanced Progress Research Agency under grant DAHC-15-73-G15, Superplastic Ultra-High Carbon Steels, Stanford University Press, by O. D. Sherby and others, Feb. 1975.

3. Taylor, J. L., Fracture Toughness of Selected Ultra High Carbon Steels, M.S. Thesis, Naval Postgraduate School, Monterey, California, 1979.

4. Chung, I., The Fatigue and Fractographic Characteristics of AISI 52100 Steel, M.S. Thesis, Naval Postgraduate School, MOnterey, California, 1979.

5. Schultz, C. W., The Effect of Thermomechanical Treatment on the Microstructure and Mechanical Properties of AISI 52100 Steel, M.S. Thesis, Naval Postgraduate School, Monterey, California, 1981.

6. McCauley, J. F., The Influence of Prior Warm Rolling on the Fracture Toughness of Heat Treated AISI 52100 Steel, M.S. Thesis, Naval Postgraduate School, Monterey, California, 1980.

7. Tufte, D. M., The Effect of Grain and Carbide Refinement on the Isothermal Transformation Characteristics of AISI 52100 Steel, M.S. Thesis, Naval Postgraduate School, Monterey, California, 1981.

8. Kar, R. J., Horn, R. M., and Zackry, V. F., "The Effect of Heat Treatment on Microstructure and Mechanical Properties in 52100 Steel," Met. Trans., Vol. 10A, Nov. 1979.

9. Metals Handbook, 8th ed., V. 4, p. 85-104, American Society for Metals, 1964.

10. Richman, R. H. and Landgraf, R. W., "Some Effects of Retained Austenite on Fatigue Resistance of Carburized Steel," Met. Trans., Vol. 6A, May 1975.

11. Krieble, R. W. and Phillip, T. V., "Effect of Retained Austenite on Copper Sulfate Corrosion Resistance of 440-C Stainless Bearing Steel," A.S.M. Materials Engr. Congress, Chicago, 1973.

12. The Timken Co., Interim Report, Influence of Retained Austenite on Compressive Properties, Contact Fatigue and Scoring Resistance of Carburized Steels, by R. Widner, 1973.

13. Rowland, E. W. and Lyle, S. R., "The Application of M_s Point to Case Depth Measurements," Trans. ASM, Vol. 37, 1946.

14. Jaffe, I. D. and Holbman, J. H., Ferrous Metallurgical Design, Wiley, 1947.

15. Leslie, W. C. and Miller, R. L., "The Stabilization of Austenite by Closely Spaced Boundaries," ASM Trans. Quart., V. 57, p. 972, 1964.

16. Woherle, H. R., Clough, H. R. and Ansell, G. S., "Athermal Stabilization of Austenite," J. Iron and Steel, 203, 1965.

17. Kinsman, K. R., Editor, "Symposium on Formation of Martensite in Iron Alloys," Trans. AIME, Vol. 12, Sept. 1971.

18. Stickles, C. A., "Carbide Refining Heat Treatments for 52100 Bearing Steel," Met. Trans., V. 5, pp. 865-874, 1974.

19. Ansell, G. S., Donachie, S. J. and Messler, R. W., "Effect of Quench Rate on the Martensitic Transformation in Fe-C Alloys," Met. Trans., V. 2, 1971.

20. SAE Report 5P-453, Retained Austenite and Its Measurement by X-Ray Diffraction, by C. F. Jatchzak and J. A. Larson, Jan. 1980.

21. Harris, W. J. and Cohen, M., "Stabilization of the Austenite-Martensite Transformation," Trans. AIME, V. 180, 1949.

22. Hanan, D. A., "Versatile 52100 Steels," The Tool and Manufacturing Engineer, Jan. 1968.

23. Gordon, P., Cohen, M. and Rose, R. S., "Effect of Quenching Bath Temperature on the Tempering of High Speed Steel," Trans. ASM, V. 33, 1944.

24. Gordon, P., Cohen, M. and Rose, R. S., "The Kinetics of Austenite Decomposition in High Speed Steel," _Trans. ASM_, March 1943.

25. Fletcher, S. G., Averbach, B. L. and Cohen, M., "The Dimensional Stability of Steel," _Trans. ASM_, Vol. 40, 1948.

26. Speich, G. R. and Leslie, W. C., "Tempering of Steel," _Met. Trans._, Vol. 3, May 1972.

27. Andrews, K. W., "Empirical Formulae for the Calculation of Some Transformation Temperatures," _JISI_, July, 1965.

28. Koistiner, D. P. and Marburger, R. E., "A General Equation Prescribing the Extent of the Austenite-Martensite Transformation in Pure Iron-Carbon Alloys and Plain Carbon Steels," _Acta Met._, Vol. 7, 1959.

29. Santiago, J. A. R., _Fracture and Fatigue Crack Growth in 52100, M-50 and 18-4-1 Bearing Steels_, Ph.D. Thesis, Massachusetts Institute of Technology, Boston, Mass., 1979.

30. Boone, D. H., Doig, A., Edwards, M. R., McNelley, T. R., and Schultz, C. W., "The Effect of Prior Heat Treatments on the Structure and Properties of Warm-Rolled AISI 52100 Steel," to be published.

31. Krauss, G., _Principles of Heat Treatment of Steel_, Publ. ASM, 1980.

INITIAL DISTRIBUTION LIST

		No. Copies
1.	Defense Technical Information Center Cameron Station Alexandria, Virginia 22314	2
2.	Library, Code 0142 Naval Postgraduate School Monterey, California 93940	2
3.	Department Chairman, Code 69Mx Department of Mechanical Engineering Naval Postgraduate School Monterey, California 93940	1
4.	Assoc. Professor Terry R. McNelley, Code 69Mc Department of Mechanical Engineering Naval Postgraduate School Monterey, California 93940	4
5.	Adj. Professor Donald H. Boone, Code 69Bl Department of Mechanical Engineering Naval Postgraduate School Monterey, California 93940	1
6.	Dr. Michael R. Edwards Metallurgy Branch The Royal Military College of Science Shrivenham, Swindon, Wilts SN6-8LA ENGLAND	1
7.	LT Steven A. Barton, USN RR 4 New London, Wis 54961	2

3 - 8

DT